PATHOLOGICAL ASPECTS AND PATHOGENESIS OF PARROT BORNAVIRUS 2 (PaBV-2) INFECTION IN PSITTACINE BIRDS

A Dissertation

by

JEANN LEAL DE ARAUJO

Submitted to the Office of Graduate and Professional Studies of
Texas A&M University
in partial fulfillment of the requirements for the degree of

DOCTOR OF PHILOSOPHY

Chair of Committee,	Aline Rodrigues Hoffmann
Co-chair,	Raquel R. Rech
Committee Members,	Ian Tizard
	J. Jill Heatley
	Susan Payne
Head of Department,	Ramesh Vemulapalli

May 2018

Major Subject: Veterinary Pathobiology

ABSTRACT

Parrot bornaviruses (PaBVs) are RNA viruses of the *Bornaviridae* family and the causative agents of proventricular dilatation disease (PDD).

PDD has many aspects that remain to be elucidated, including the mechanisms involved in its pathogenesis. The purpose of this work was to investigate different hypotheses linked to the pathogenesis of Parrot bornavirus 2 (PaBV-2) infection in psittacine birds.

We first tested the hypothesis of antibodies against gangliosides being involved in the development of PDD in psittacine birds. We analyzed the relationship between the presence of antiganglioside antibodies and microscopic lesions related to PDD in birds. No association between the presence of anti-ganglioside antibodies and the development of lesions resembling PDD was observed in our study, which corroborates with the hypothesis that PDD is not an auto-immune disease as previously speculated.

Second, we analyzed the progression of viral antigen and inflammatory lesions after the intramuscular inoculation of PaBV-2 in cockatiels. Histopathological, immunohistochemical and molecular analyses were performed in tissues of cockatiels in a chronological fashion. PaBV-2 was first detected in leukocytes in the inoculation site and adjacent nerves, then reached the brachial plexus, centripetally spread to the thoracic segment of the spinal cord, and subsequently invaded the other spinal segments and brain. PaBV-2 then centrifugally spread out of the central nervous system (CNS) to peripheral ganglia. Our results demonstrate that PaBV-2 first targets the CNS, before migrating to peripheral tissues such as the GI system.

Finally, we aimed to evaluate the distribution of inflammatory foci and viral antigen throughout 4 selected levels of brain and 3 segments of spinal cord in cockatiels experimentally infected with PaBV-2. Immunolabeling was first observed in the ventral horns of the thoracic spinal cord. Inflammatory lesions were first identified in the gray matter of the thalamus and brainstem. Encephalitis was more severe in the thalamus and brainstem, while myelitis was equally distributed between all segments of the spinal cord. Our results demonstrate a caudal-rostral viral distribution of PABV-2.

Our results reemphasize the role of PaBVs as the causative agents of PDD; the lack of an autoimmune component; and the detection of PaBV-2 in the CNS before peripheral organs.

DEDICATION

To all birds that participate in this study. Thank you.

I sincerely hope our results can help understanding this devastating disease and contribute for the conservation of many species.

ACKNOWLEDGEMENTS

I would like to thank my committee chair, Dr. Rodrigues Hoffmann and my co-advisor Dr. Raquel Rech, for believing in me even when I lost faith in myself. This study would not be possible without their phenomenal, and sometimes maternal, guidance.

I would like to also thank my committee members, Dr. Tizard, Dr. Heatley, and Dr. Payne, for their guidance and support throughout the course of this research.

Thanks also to Courtney Smith, Caitlin Older, Paula Giaretta, Anna Blick and Alex Myers for being the best lab mates and friends I could have asked for.

Thanks also to all faculty and staff for making my time at Texas A&M University a great experience.

Thanks to CAPES - Science without borders program that allowed me to do my PhD at Texas A&M University.

Finally, thanks to my mother and father for the gift of life.

CONTRIBUTORS AND FUNDING SOURCES

This work was supervised by a dissertation committee consisting of Professor Aline Rodrigues Hoffmann, advisor, Professor Raquel R. Rech, co-advisor, and Professors Ian Tizard and Susan Payne of the Department of Veterinary Pathobiology, and Professor J. Jill Heatley of the Department of Small Animal Clinical Sciences. All work for the dissertation was completed independently by the student.

We would like to also thank the Open Access to Knowledge Fund (OAKFund) for supporting the publication of the manuscripts originated from this dissertation.

This study was supported by the Science without Borders fellowship and by the Schubot Avian Health Center and Department of Veterinary Pathobiology at Texas A&M University.

NOMENCLATURE

PaBV	Psittaciform 1 bornavirus
PaBVs	Parrot bornaviruses
PaBV-2	Parrot bornavirus 2
PDD	Proventricular dilatation disease
IHC	Immunohistochemistry
IIFA	Indirect immunofluorescence assay
ELISA	Enzyme-linked immunosorbent assay
H&E	Hematoxylin and eosin
RNA	Ribonucleic acid
mRNA	Messenger ribonucleic acid
PCR	Polymerase Chain Reaction
qPCR	Real-time polymerase chain reaction
GBS	Guillain-Barre syndrome
CNS	Central nervous system
PNS	Peripheral nervous system
DPI	Day post-inoculation
RNP	Ribonucleoprotein

TABLE OF CONTENTS

Page

LIST OF FIGURES

Page

LIST OF FIGURES

Page

LIST OF TABLES

Page

CHAPTER I

INTRODUCTION AND LITERATURE REVIEW

Bornaviruses

Bornaviruses are enveloped, non-segmented, single stranded, negative sense, RNA viruses with an 8.9 Kb genome.[1] These viruses belong to the order Mononegavirales, family *Bornaviridae* and to the genus Bornavirus. As observed in table 1, this monogeneric family contains 8 species that encompasses 16 viruses, besides 4 unclassified viruses that need more genetic evidence to be recognized as new species. Two species have been identified in mammals (Mammalian 1 bornavirus and Mammalian 2 bornavirus); Five species can infect birds (Psittaciform 1 bornavirus, Psittaciform 2 bornavirus, Passeriform 1 bornavirus, Passeriform 2 bornavirus and Waterbird 1 bornavirus) and 1 species has been recognized in reptiles (Elapid 1 bornavirus).[2,3]

The Bornaviral genome encodes 6 viral proteins: nucleprotein (N), phosphoprotein (P), matrix protein (M), glycoprotein (G), polymerase (L) and a nonstructural regulatory protein named X protein. Bornaviruses use the RNA splicing machinery for gene expression, which maximizes the use of the genome.[4] N, P and L proteins together with the viral RNA form a viral ribonucleoprotein (RNP) complex, which is transmitted between cells.[5] Once in the cytoplasm, the RNP complex is transported to the nucleus, where viral replication and transcription take place. The mechanisms used by the bornaviral RNP to be exported from the cell are still unclear.[6,7] Only small numbers of infectious particles are released from infected cells.[4]

Table 1. Taxonomy of bornaviruses

Order	Family	Genus	Species	Virus
Mononegavirales				
	Bornaviridae			
		Bornavirus		
			Mammalian 1 bornavirus	
				borna disease virus 1 (BoDV-1)
				borna disease virus 2 (BoDV-2)
			Mammalian 2 bornavirus	
				variegated squirrel bornavirus 1 (VSBV-1)
			Psittaciform 1 bornavirus	
				parrot bornavirus 1 (PaBV-1)
				parrot bornavirus 2 (PaBV-2)
				parrot bornavirus 3 (PaBV-3)
				parrot bornavirus 4 (PaBV-4)
				parrot bornavirus 7 (PaBV-7)
			Psittaciform 2 bornavirus	
				parrot bornavirus 5 (PaBV-5)
			Passeriform 1 bornavirus	
				canary bornavirus 1 (CnBV-1)
				canary bornavirus 2 (CnBV-2)
				canary bornavirus 3 (CnBV-3)
			Passeriform 2 bornavirus	
				estrilid finch bornavirus 1 (EsBV-1)
			Waterbird 1 bornavirus	
				aquatic bird bornavirus 1 (ABBV-1)
				aquatic bird bornavirus 2 (ABBV-2)
			Elapid 1 bornavirus	
				Loveridge's garter snake virus 1 (LGSV-1)
			Tentative, unclassified bornaviruses	
				Gaboon viper virus 1 (GaVV-1)
				munia bornavirus 1 (MuBV-1)
				parrot bornavirus 6 (PaBV-6)
				parrot bornavirus 8 (PaBV-8)

One important difference between the avian and mammalian bornaviruses is that avian bornaviruses lack the short open reading frame segment in the 5' noncoding region of the bicistronic mRNA that encodes the X and P proteins of mammalian bornaviruses.[8] This suggests that other mechanisms are involved in the regulation of these 2 proteins.

Briefly, the replication cycle of Bornaviruses consists of: [9,10]

1. Bornaviruses initiates attachment via binding of its envelope glycoprotein (G) to unidentified cellular receptors;
2. Virus enters cells by receptor-mediated endocytosis;
3. Fusion between the cell and viral membranes is mediated by the acidic environment of the late endosome, which releases the RNP into the cell cytoplasm;
4. Viral RNPs are transported to the nucleus by unknown mechanisms;
5. Viral replication and gene transcription takes place in the nucleus;
6. Newly synthetized viral RNPs and the viral surface glycoproteins exit the nucleus;
7. RNPs participate in the budding process and are incorporated into viral particles.

Bornaviruses are non-cytopathic in cell culture,[11] and establish non-cytolytic persistent infections in their hosts.[12] Among the animal RNA viruses, only three taxa can replicate in the nucleus: The families *Bornaviridae*[13] and *Orthomyxoviridae,*[14] and also the Nyamanini virus (Family *Nyamiviridae*),[15] however, since Bornaviruses are the only

one of these taxa to have a non-cytolytic nature, they are the only known RNA viruses to establish a persistent infection in the host nucleus.[12]

Parrot bornaviruses and proventricular dilatation disease

Initially described in the late 1970s and early 1980s as a disease of large psittacine birds, and therefore originally named "macaw wasting syndrome", proventricular dilatation disease (PDD) is a fatal and important disease of psittacine birds worldwide, however, its cause remained obscure for many decades.[16,17]

In 2008, two independent studies identified a group of enveloped, non-segmented, negative sense single-stranded RNA viruses of the *Bornaviridae* family as the cause of PDD.[18, 19] This virus was initially named avian bornavirus, but further molecular investigation revealed a diverse group of viruses.[20-24] The discovery of this high genetic variability of avian bornaviruses associated with the identification of the Variegated squirel bornavirus 1 (VSBV-1),[25] caused an important rearrangement in the monogeneric family *Bornaviridae*, which was reorganized in 2015 to incorporate 8 distinct species of mammalian, reptile and avian, besides unclassified and unassigned bornaviruses. Eight viruses have been identified in psittacine birds, named parrot bornavirus 1 to 8 (PaBV-1 to PaBV-8). Five of these viruses (PaBV-1 to 4, PaBV-7) belong to the species Psittaciform 1 bornavirus, whereas PaBV-5 is a member of the species Psittaciform 2 bornavirus, and PaBV-6 and PaBV-8 remain unclassified.[3, 26]

These bornaviruses can affect a broad range of tissues and cell types, however, neurotropism is a pronounced feature, which is reflected by a lymphoplasmacytic

meningoencephalomyelitis and ganglioneuritis (remarkably prominent in the enteric nervous system),[27-29] especially in psittacine birds. These lesions may give rise to neurologic or gastrointestinal signs, or even a combination of both, including lethargy, depression, ataxia, regurgitation, emaciation and impairment in digestion,[19, 30-32] therefore, clinical presentation of PDD is markedly variable and recent studies suggest that different parrot bornaviruses (PaBVs) can cause different patterns of PDD lesions and clinical disease, with predominant neurological or predominant gastrointestinal presentations.[32] The development of the disease is also particularly variable, ranging from acute death to slow progression of clinical disease and not all infected psittacine birds develop clinical disease.[32-34]

Despite the intensive efforts on PDD research, the pathogenesis of this condition and how PaBV causes disease, remains unclear. Several studies were able to reproduce clinical disease and classical lesions of PDD after experimental inoculation of PaBVs, and were also able to recover this virus from birds that developed the disease, which fulfills Koch's postulates and reaffirms PaBVs as the putative agents of PDD in psittacine birds.[17,35,36,37]

Avian bornaviruses have been identified worldwide, including countries such as the United States, Canada, Brazil, South Africa, Austria, Germany, Spain, United Kingdom, Italy, Denmark, Australia, and Japan.[38] Psittaciform 1 and 2 bornaviruses affect different species of psittacine birds, such as amazon and grey parrots, macaws, cockatoos, cockatiels, and conures. While, passerine birds and waterfowl harbor their own avian

bornaviruses, which are members of the species *Passeriform 1* and *2 bornaviruses* and *Waterbird 1 bornavirus*, respectively.[17, 26, 39]

Pathogenesis of mammalian bornaviral infections

In mammals, three pathogenic processes cause neuronal damage associated with bornaviral infection.[4] First, the virus replicates almost exclusively in neurons which triggers immune-mediated attack by CD8+ T cells directed against viral antigens such as the bornaviral N-protein.[40] These T-cells mount a Th-1 response characterized by the production of both IFN-γ and TNF-α. It has been reported that in bornaviral lesions, the perivascular infiltrates are predominantly CD4+ T cells, whereas the infiltrate in the brain parenchyma is composed of CD8+ T cells. The neurotransmitters glutamine and acetylcholine also favor T cell activation.[41,42,43]

Immunosuppressive studies strongly support the crucial role of T cells in bornaviral pathogenesis. It has been demonstrated that T cell elimination prevented inflammation and development of clinical disease and administration of immunosuppressive drugs such as cyclophosphamide and cyclosporine prior to infection, was able to prevent bornaviral disease in rats. [44,45,46, 47] However, adult rats infected with BoDV-1 only show the virus in the brain, while immunosuppressed infected rats also show the virus in peripheral nervous system and other tissues, such as liver and lungs, suggesting that T-cells have an essential role containing the virus in the central nervous system.[48,47]

Studies following the immune response in the brain of BoDV-1 infected Lewis rats have been important to demonstrate the participation of cytokines and inflammatory cells

in bornaviral infections.[49] NK cells could be identified in the brain lesions 3.5 weeks after inoculation and before any clinical signs. The chronicity of the disease was accompanied by a reduction in the number of all cell types, and this phenomenon was interpreted as a switch from a type 1 to a type 2 immune response, also supported by a rise in IgE levels. Pro-inflammatory cytokines, such as IL-1α, IL-2, IL-6, TNF-α and IFN-γ were increased and peaked at 5 weeks post-inoculation, whereas IL-4, an anti-inflammatory cytokine, reached the maximal levels at 15 weeks post-inoculation. It has been also suggested that the reduction of inflammation in long-term bornaviral infections is also due to the neuroprotective effects of Treg cells.[50]

In the late stages of infection, the virus infects microglia and astrocytes, which leads to prolonged activation of microglia and increased release of cytokines and reactive nitrogen species. Microglia normally remodel neuronal synapses and secrete neurotrophic proteins; however, they release inflammatory cytokines and induce nitric oxide synthase (iNOS), reactive oxygen species (ROS) and reactive nitrogen species (RNS) when activated. These molecules can be associated with neuronal dysfunction and death. In the experimental rat model of bornaviral encephalitis, it has been demonstrated the close association between the severity of the neurological signs and the iNOS and cNOS mRNA expression. Furthermore, the distribution of iNOS-positive cells in the basolateral cortex and the hippocampus correlates with the location of BoDV-1 infected cells. However, one study has demonstrated that mice lacking IFN-γ, Fas, iNOS and CXCR3 were not prevented from developing neurological disease. [51,52,53,54]

Similar to other tissue-resident macrophages, classically activated microglia (M1 cells) can be differentiated into regulatory cells (M2 cells), therefore reducing inflammation and promoting tissue repair, or they can undergo uncontrolled activation, which triggers chronic inflammation and results in the production of neurotoxic factors and progressive neuronal loss. In rats, there is supportive evidence that microglia directly mediate pro-inflammatory cytokines in bornaviral disease.[49]

Finally, it is reported that astrocyte dysfunction due to viral invasion disrupts glutamate regulation and glutamate excess ultimately kills neurons through excitotoxicity. Astrocytes are the major glial cell population in the brain and among their various functions, they remove excess neurotransmitters such as glutamate. Astrocytes take up extracellular glutamate, and transform it into glutamine using glutamine synthetase. [55,56]Glutamate has an essential role associated with excitatory synaptic transmission, however if the extracellular concentration of gluatamate is excessive, this will damage the neurons. It has been demonstrated that cats and rats infected with BoDV-1 have a dysfunction in the glutamate removal by astrocytes and consequently increased levels of glutamate. Furthermore, T cells have receptors for glutamate, and glutamate is associated with the increase of T cell adhesion, chemotactic migration, proliferation and protection against antigen-induced apoptosis. Therefore, glutamate increase produced by Bornavirus-induced astrocyte dysfunction, may attract T cells and promote T-cell-mediated brain damage.[57]

Additionally, bornaviral P-protein has been suggested to bind directly to Gamma-aminobutyric acid (GABA) receptors, and that BoDV-1 could interfere with the GABA-

glutamate cycle reducing its inhibitory function and increasing excitotoxicity and T cell activity. It has been recognized that Bornavirus also has effects on cholinergic activity and dopamine system, besides disruption of several molecular pathways such as NF-kβ and RIG-1/MAVS.[58,59]

Furthermore, it has been suggested that, similar to infections by large DNA viruses, BDV infection could be accompanied by virus mediated change in the host cell epigenome.[4] It has been demonstrated that BDV P protein inhibits cellular histone acetyltransferase activities and consequently modulates viral replication.[60]

In rodents, BoDV-1 has a pronounced neurotropism for the limbic system and the main affected areas in the brain are the olfactory bulb, the dentate gyrus, the caudate nucleus, the hippocampus, mesencephalon, central gray matter, substantia nigra and hypothalamus which are characterized by lymphoplasmacytic infiltrates.[61,62] In horses, sheep, and humans the highest viral titers and more prominent inflammatory lesions are in the piriform cortex and hippocampus.[40] In cats with bornaviral staggering disease, the lesions are similar to the ones observed in horses and sheep, but plasma cells may be more prominent.[63] There are no studies with a consistent lesion distribution and viral presence in the brain of avian species.

Pathogenesis of avian bornaviral infections

Several key mechanisms of bornaviral infection pathogenesis in psittacine birds are still unclear, including natural route of infection, receptors, and cells involved in the infection pathways. Bornaviral infections have been experimentally reproduced in several

studies,[17, 31, 32, 35-37, 64] using different species as experimental models, including cockatiels, conures and canaries. In these studies, routes of infection of psittacine birds consisted of single intramuscular, intravenous or intracerebral routes[17, 32, 36] or using different protocols of intramuscular, oral, oculonasal, and subcutaneous routes combined[31, 35, 37, 64]. Recently, a study involving cockatiels inoculated by intranasal or oral routes failed to induce PaBV infection or to induce PDD lesions in any of the birds during 6 months of experiment[65], suggesting that these routes are unlikely to be involved in natural PaBV infection.

In these experimental studies, clinical signs induced after inoculation of PaBVs included weight loss, undigested seeds in the feces, regurgitation, weakness, anorexia, diarrhea, ataxia, and sudden death. The first time point of clinical signs ranged from 21 to 92 dpi, and in the majority of the studies, gastrointestinal signs have been observed before neurological signs.[17, 31, 32, 36, 66]

Serological investigation of PaBV-infected birds has been performed in several studies using Western blot, ELISA, and indirect immunofluorescence assay (IIFA) for detection of the PaBV-specific proteins, P40 (N protein), P24 (P protein), and/or P16 (M protein) or evaluation of antibodies targeting these proteins.[30, 67-69] Using ELISA, antibodies against P40 are the most frequently detected in these studies, although variable measurements have been reported for different species of psittacine birds infected with PaBVs. Recent studies have demonstrated that not all birds expressing PaBV-protein specific antibodies demonstrate clinical signs, suggesting a high number of asymptomatic PaBV-carriers.[67] Some investigations using Western blot have shown that between 82 to 94% of PDD-infected birds are reactive to a 38-40 KDa protein consistent with PaBVs N-

protein, while approximately 15% of apparently healthy birds also reacted to this protein, reinforcing the hypothesis of asymptomatic carriers.[68] Serological techniques have also been attributed to be more sensitive for the detection of PaBV infections than molecular techniques, since the high genetic variability of different PaBVs species can interfere in the RT-PCR results. For instance, studies using indirect immunofluorescence assay (IIFA) for the detection of, were able to detect PaBV- specific antibodies in 45% of infected psittacine birds, while PaBV RNA was only amplified in only 36% of these birds.[69]

Despite the strong evidence of the causal association of PaBV and PDD, several aspects of its pathogenesis are still unclear. First, in some studies not all infected birds developed clinical disease and died, and in fact some have become healthy carriers after experimental inoculation.[70, 71] Secondly, although the published studies report when the birds show the first clinical signs after experimental inoculation of PaBV, they do not show a careful and detailed description of viral and lesion distribution in the multiple organs that can be affected in PDD cases. This crucial information of the PDD pathogenesis remains to be elucidated.

Pathological aspects of PDD and bornaviral infections in birds have been reported since the 1980s.[16, 72] Macroscopic alterations are restricted to the GI system and can be seen as a thin-walled dilation of the crop, proventriculus, ventriculus and/or small intestine. However, as the name of the disease suggests, the dilation of the proventriculus is the most frequent gross finding observed in natural and experimental cases of PDD. Histologically, lymphoplasmacytic infiltrates in gastrointestinal, adrenal, and epicardial ganglia and nerves have been consistently reported in PDD cases. Additionally, these same

infiltrates can affect the CNS of infected birds, predominantly forming perivascular cuffing in the gray matter of brain and spinal cord, and have been extensively described in the literature.[73-75]

Immunohistochemistry has been widely implemented as an ancillary test for the identification of PaBVs antigen in tissues. Antibodies against PaBV's N and P proteins have been the most common used IHC antibodies in a variety of studies involving experimental and natural PaBV infections. Immunolabeling can be observed in the nucleus, or nucleus and cytoplasm, of infected neurons, ependymal and glial cells in the cerebrum, cerebellum, brainstem and spinal cord, additionally, in neurons and Schwann cells in peripheral ganglia and nerves of multiple tissues including crop, esophagus, proventriculus, ventriculus, small and large intestine, heart and adrenal gland are immunolabeled. There are also reports of occasional immunolabeling in smooth muscle cells of the GI tract, cardiomyocytes, tubular epithelial cells of the kidneys, epithelial cells of proventriculus and duodenum, pancreatic islet cells, photoreceptors in the retina and medullary cells of the adrenal glands. Due the intranuclear replication of bornaviruses, immunolabeling only in the cytoplasm of cells has been consistently interpreted as spurious immunoreactivity and not associated with PaBV antigen.[73, 74, 76, 77]

Although well documented lesions and immunohistochemistry results of PaBV-infected birds have been reported in the last decades, a more thorough description of the main affected areas in the CNS and PNS are still required in order to elucidate some key aspects of the pathogenesis of this disease.

CHAPTER II

ANTI-GANGLIOSIDE ANTIBODIES AND PROVENTRICULAR DILATATION DISEASE[1]

Introduction

Several mechanisms have been proposed to explain how PaBVs causes ganglioneuritis as well as the encephalomyelitis in birds.[17, 39] The pathogenesis of PDD has been linked to two main hypotheses: the first and most accepted theory states that PaBVs spread throughout the nervous system and directly triggers the inflammatory and immunological changes that lead to damage in the CNS, the enteric nervous system and peripheral nerves.[32] The second hypothesis proposes the pathogenesis of PDD in psittacine birds is caused by the production of autoantibodies targeting components of the nervous system, [78] a similar mechanism to an autoimmune condition of humans called Guillain–Barré syndrome (GBS).

GBS is the most common cause of acute flaccid paralysis in humans since the near eradication of poliomyelitis.[79] The disease results in a demyelinating neuropathy that affects the PNS and causes symmetrical limb weakness that may lead to paralysis in 2 to 3 weeks.[80] The pathogenesis of GBS and other autoimmune diseases such as, acute disseminated encephalomyelitis and neuromyelitis optica, is associated with molecular

[1] Reprinted with permission from "Are anti-ganglioside antibodies associated with proventricular dilatation disease in birds?" by Leal de Araujo J, Tizard I, Guo J, Heatley JJ, Rodrigues Hoffmann A, Rech RR, 2016. PeerJ, 5, 83-87, Copyright 2016 by Leal de Araujo et al.

mimicry. In this case, bacteria (e.g. *Campylobacter jejuni*) or viruses (e.g. Cytomegalovirus, Zika virus, Chikungunya virus, Epstein-Barr virus) mimic the structure of a specific host antigen and so triggers an immune reaction against tissue containing the cross-reacting antigen, such as neuronal gangliosides.[81-84] These complex glycosphingolipids are expressed in abundance on neurons of the CNS and PNS,[85] and have an important role in cellular interactions. When targeted by auto-antibodies, neuronal damage occurs, leading to the development of GBS.[86]

This study aimed to evaluate the relationship between the experimental inoculation of gangliosides or crude nervous tissues and the development of neurologic disease in chickens (*Gallus gallus domesticus*) and PaBV-free quaker parrots (*Myiopsitta monachus*) that could resemble PDD.

Material and methods

Experimental design

Two experiments were performed. The first experiment aimed to analyze whether or not the inoculation of gangliosides in an avian species (chickens) could lead to the development of neurological or gastrointestinal signs that could resemble PDD. Only histologic examination was performed in this experiment. A second experiment was performed in order to determine if the inoculation of crude nervous tissue or purified gangliosides in a psittacine species (quaker parrots) could lead to neurological or gastrointestinal disease, resembling those seen in cases of PDD. In this experiment, blood

samples were collected in order to evaluate anti-ganglioside antibody and fibrinogen levels. Samples were also collected for histologic examination.

Inoculum preparation and purification

Gangliosides were extracted from brain, spinal cord, sciatic and brachial nerves, and nerve of Remak from ten healthy chickens, and three healthy PaBV-free quaker parrots, using a modified technique[87] adapted for this purpose by Pesaro.[88]

Thin layer chromatography (TLC)

The isolation of brain gangliosides was confirmed using a thin-layer chromatography (Scandroglio *et al.*, 2009). Given the lack of commercially available avian gangliosides, a bovine ganglioside mixture (Millipore, Billerica, MA) was used as the standard for the TLC analysis. The solvent system utilized for this purpose was composed of 50:42:11 volume of chloroform/methanol/0.2% aqueous $CaCl_2$. After separation, gangliosides were stained using Ehrlich's reagent, prepared with 6 g of p-dimethylaminobenzaldehyde in 50 ml of 37% hydrochloric acid and 50 ml of 95% ethanol.

Experimental animals

The experiments described here were performed under animal use protocol number IACUC 2014-0006, approved by the Texas A&M University Institutional Animal Care and Use Committee. To determine if the inoculation of brain gangliosides into an avian species could induce neurologic disease, we performed a preliminary study using 17 healthy female, white, leghorn chickens, between 10 to 15 weeks old, and vaccinated for

Marek's disease originated from Texas A&M University Poultry Science Center, which were divided into 2 groups: The first group was comprised of 11 chickens (C1 to C11), inoculated with 1 ml of purified gangliosides and FCA in the pectoral muscle. The second group consisted of 6 chickens (C12 to C17) inoculated only with phosphate-buffered saline (PBS) and served as controls. All chickens were inoculated twice with 31 days between each inoculation, as performed before by Pesaro, 2008. The chickens that did not present clinical signs were euthanized 62 days post inoculation (dpi).

The second experiment included 5 healthy adult quaker parrots (*Myiopsitta monachus*) selected from a colony tested for PaBV every 3 months by RT-PCR and Western blot, as previously described,[89] and were consistently negative at all times. The quaker parrots were divided into 3 groups and a solution was injected in the pectoral muscle, as follows: group 1, one quaker parrot (QP1) was inoculated with 0.5 ml of FCA (negative control); group 2, two quaker parrots (QP2 and QP3) were inoculated with 0.5 ml of an emulsion of FCA and purified quaker brain gangliosides; and group 3 (QP4 and QP5) consisted of two quaker parrots inoculated with 0.5 ml of an emulsion of FCA and crude nervous extracts (mixture of brain, spinal cord, sciatic, and brachial nerves, and nerve of Remak). All quaker parrots were inoculated three times, with 24 days interval between each inoculation and euthanized at 83 dpi (Figure 1). In contrast to the chickens, an additional inoculation was performed in the quaker parrots in order to stimulate the production of antibodies and consequently lesions. All animals in this experiment were anesthetized with Isofluorane and then euthanized with carbon dioxide (CO_2). All birds were clinically evaluated daily and any abnormal signs (particularly neurological or

gastrointestinal signs) or behavior were documented. Blood samples from quaker parrots were collected at different time points for Western blot, ELISA and fibrinogen determination (Figure 1).

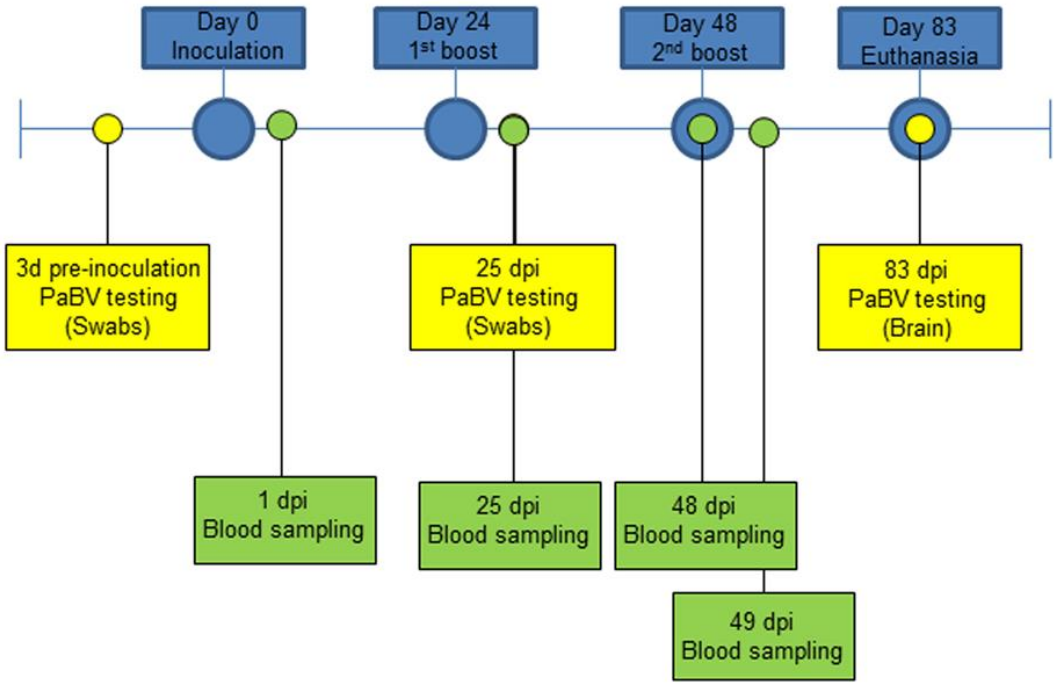

Figure 1. Experiment timeline for quaker parrots. They were divided into 3 groups and inoculated 3 times with 0.5 ml of three different preparations (Purified gangliosides + Freund's adjuvant; Crude nervous tissues + Freund's adjuvant; or only Freund's adjuvant) with 24 days between each inoculation. RT-PCR for PaBV was performed from cloacal swabs at 3dpi, 25 dpi and from brain at 83 dpi. Blood samples were collected at 1 dpi, 25 dpi, and 48 dpi and were used for serological and fibrinogen analysis, and at 49 dpi to evaluate fibrinogen levels following the second ganglioside inoculation.

RT-PCR

The quaker parrots used in this experiment were further tested for PaBV by RT-PCR. Cloacal and choanal swabs were collected for RT-PCR 3 days before inoculation and 25 dpi. Samples from brain, spinal cord and nerves were also collected during necropsy at 83 dpi and tested by RT-PCR. Briefly, RNA was extracted from samples using a QIAamp® Viral RNA Mini Kit (Qiagen,Valencia,CA) and reverse-transcribed and amplified using primers targeting the PaBV matrix gene, as previously described (Guo et al., 2014). Positive and negative samples from other psittacine birds not related to this study were used as positive and negative controls. The amplification products were analyzed by a 1.5% agarose gel electrophoresis. The nervous tissues used for the preparation of the inoculum were also tested by RT-PCR for PaBV prior to inoculation into the quaker parrots.

Fibrinogen assessment

Plasma samples from quaker parrots were submitted to the Clinical Pathology laboratory at the Veterinary Medicine Teaching Hospital at Texas A&M University for measurement of fibrinogen concentrations using the heat precipitation method as previously described.[90] Samples were collected at 1 dpi, 25 dpi, 48 dpi and 49 dpi (Figure 1).

Pathology

A systematic necropsy was performed on all birds and representative tissues of CNS, PNS, gastrointestinal tract, skin, musculoskeletal, endocrine and genitourinary systems were collected and processed for routine histological examination.

Serology

Quaker parrot sera were evaluated for reactivity against the crude and purified extracts used for inoculation by Western blot. This technique was performed based on previously described methods.[89, 91] Briefly, crude and purified extracts were mixed with gel loading buffer and electrophoresed on 10% polyacrylamide gels. Proteins were transferred to a polyvinylidene fluoride (PVDF) membrane in transfer buffer at 100 mA for 2 hours. Membranes were incubated in blocking solution at room temperature for 2 hours and then cut into strips and incubated for 2 hours with each individual bird serum diluted 1:1000 in blocking solution and acting as the primary antibody. The membrane stripes were then incubated with alkaline phosphatase labeled goat anti-macaw IgY antibody diluted 1:5000 in blocking buffer for 1 hour. Membranes were rinsed and stained with 5-bromo-4-chloro-3-indolyl phosphate/p-nitroblue tetrazolium chloride (BCIP/NBT) (Sigma-Aldrich, St.Louis, MO).

Measurement of anti-gangliosides antibodies was performed using enzyme-linked immunosorbent assay as previously described,[92] with minor modifications for use with bird serum. Sera from 1 dpi, 25 dpi and 48 dpi from each quaker parrot was analyzed by ELISA and a healthy macaw serum was also used as negative control. Microtiter plates

were coated with 100 µl per well of the crude or purified extracts in triplicate, and incubated at 4°C overnight. Following incubation, wells were blocked with 5% fat-free dried milk in PBST for 1 hour. Serum from each bird was diluted 1:5000 and added to the wells and incubated for 1 hour at room temperature. After three washes of PBST, the plates were incubated for 1 hour with 100 µl of anti-macaw IgY antibody. TMB (3,3', 5,5;-tetramethylbenzidine) substrate (Invitrogen, Carlsbad, CA) was added and incubated for 15 min. Sulfuric acid (H_2SO_4) was used to stop the reaction and optical density (OD) was measured at 450 nm. Sera with absorbance values higher than 0.1 were considered positive.

Results

Thin Layer Chromatography (TLC)

Using a solvent system comprised by chloroform/methanol/0.2% aqueous $CaCl_2$ 50:42:11 volume, we were able to separate the aqueous phase of the inoculum demonstrating the presence of gangliosides when compared to the standard bovine ganglioside mixture. Using Ehrlich's reagent, gangliosides reacted as grey spots on the TLC plate.

Clinical signs

Chicken C1 presented with mild walking difficulty and weakness at 14 dpi and was euthanized. All of the other chickens remained healthy and were euthanized at the end of the experimental period at 62 dpi. None of the quaker parrots presented clinical signs

that resembled PDD (i.e. undigested seeds in the feces, regurgitation, neurological signs) or a peripheral neuropathy that could resemble GBS. However, nonspecific signs such as mild depression (QP2 and QP5) and weight loss (QP4) were observed.

PaBV-RT-PCR

All quaker parrots tested negative for PaBV on cloacal and choanal swabs by RT-PCR 3 days before inoculation and 25 dpi. Samples collected from the brain, spinal cord and nerves from all quaker parrots at time of euthanasia, as well as the inoculum used to inject the birds, were negative for PaBV by RT-PCR.

Fibrinogen analysis

Fibrinogen levels, an important inflammatory marker in birds, were increased in QP5, 24 hours after each inoculation, reaching levels up to 400mg/dL (Table 2). QP2, QP3, QP4 had variable fibrinogen levels, with the highest levels at 49 dpi. The fibrinogen levels for control QP1 were less than 100mg/dL throughout the study.

Table 2. Fibrinogen levels (mg/dL) in quaker parrots measured at 4 different timepoints.

QP#	1 dpi	25 dpi	48 dpi	49 dpi
1	<100	<100	<100	100
2	<100	100	<100	200
3	<100	<100	<100	400
4	100	<100	100	400
5	200	300	300	400

Serology

The Western blot using the crude extract showed fewer bands from the sera from the quaker parrots inoculated with the purified ganglioside extract (QP2 and QP3) and several nonspecific bands for the birds inoculated with the crude extract (QP4 and QP5) (Figure 2). The Western blot from control QP1 did not present any bands. The blots loaded with the purified extract only reacted with the sera of the birds inoculated with the purified extract, showing fewer faint bands when compared to the crude extract blots. A 45 kDa band was observed in the blots from QP2 and QP3, which were treated with purified gangliosides. This is the molecular weight of ganglioside binding proteins.[93]

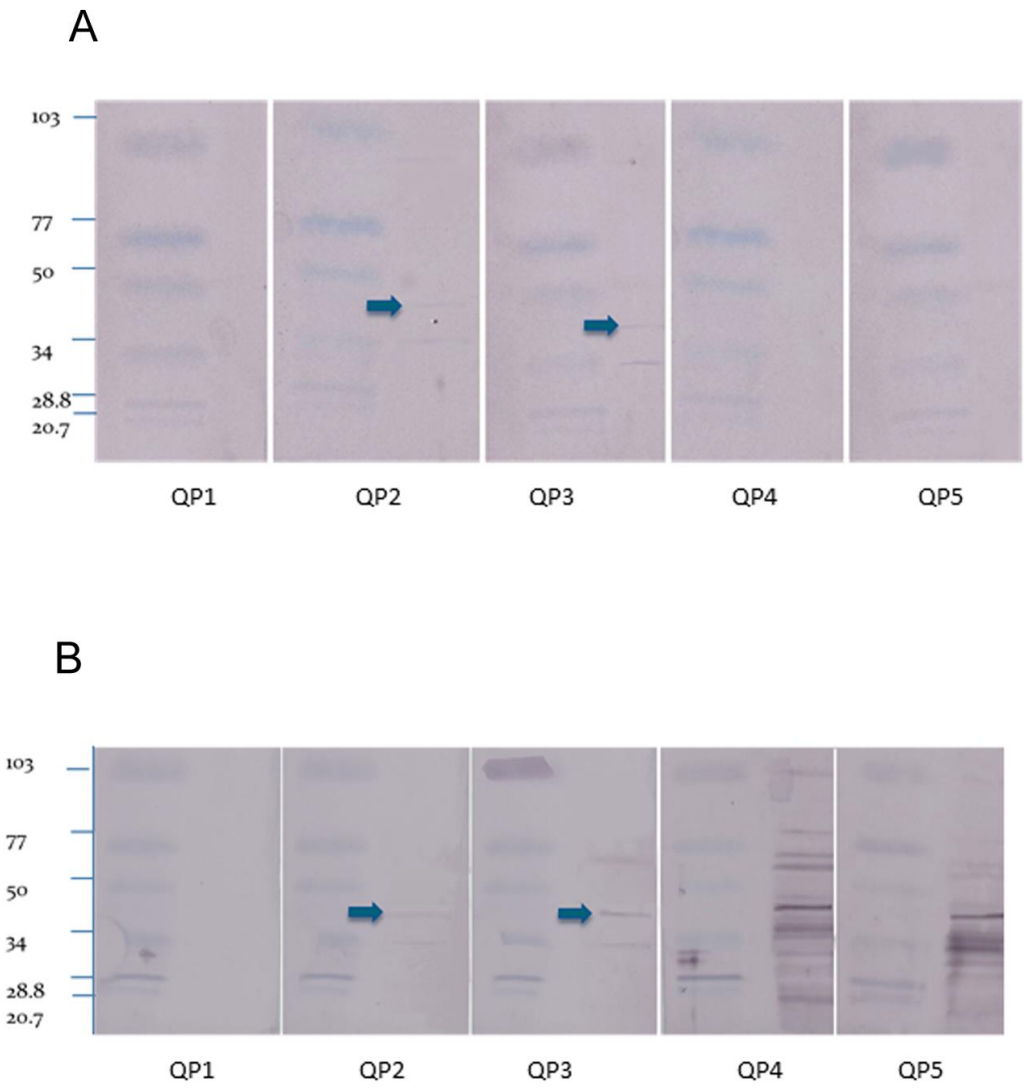

Figure 2. Western blot. Purified (A) and crude (B) nervous extracts exposed to sera from 5 different quaker parrots. Bird 1 was inoculated only with Freund's adjuvant and served as control. Quaker parrots 2 and 3 were inoculated with purified gangliosides and quaker parrots 4 and 5 were inoculated with crude nervous tissue extracts. Quaker parrots 2 and 3 presented bands with approximately 45 kD (arrows), while the crude extract blots presented several unspecific bands when exposed to QP4 and QP5 sera.

All inoculated quaker parrots (QP2 to QP5) presented a marked increase in the absorbance values on ELISA (Figure 3) using the purified and crude ganglioside extracts when comparing the first timepoint to the second and third timepoints. Due to the lack of a positive control originated from a quaker parrot with proved anti-ganglioside antibodies, the ELISA evaluation was performed based on the exposure of QP1 serum to the crude and purified extracts and also the serum from a healthy macaw exposed to these extracts. For the plates coated with the purified extract, QP2 had absorbance values, almost 2 times higher than sera from QP1, when comparing the second and third timepoints. The plates coated with crude extract, QP4 had absorbance values from the second and third timepoints almost 3 times higher when compared to QP1 (control). The sera from QP1 and the healthy macaw sera had constant low values at all 3 timepoints for plates coated with purified and crude extracts.

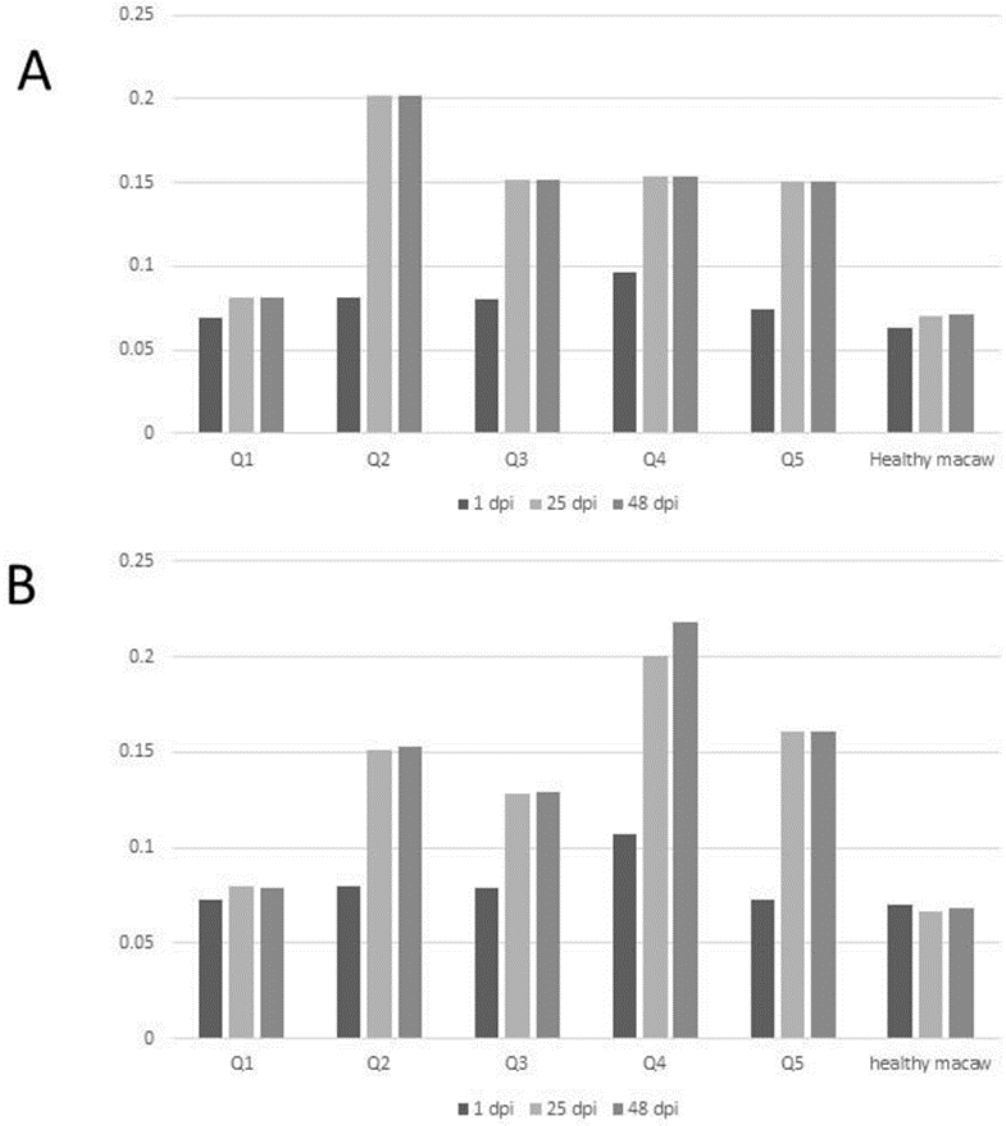

Figure 3. Enzyme-linked immunosorbent assay. Variability of auto-ganglioside antibodies of each quaker parrot serum measured by ELISA for three different timepoints. **A.** Plate coated with purified gangliosides. **B.** Plate coated with crude extracts. The vertical axis demonstrates the absorbance readings values at 450 nm. A healthy macaw serum was used as a negative control.

Pathology

Chicken C1 (euthanized at 14 dpi) had an intense inflammatory reaction in the site of the inoculation in the pectoral muscle. No gross lesions were observed in any of the quaker parrots. Histologically, C1, presented with a mild perivascular and perineural lymphocytic infiltrate in the proventriculus, while C5, and C6 presented with minimal to mild, focal, lymphocytic aggregates in the cerebrum. QP2 had a mild, multifocal, lymphoplasmacytic encephalitis in the optic tectum (Figure 4A). QP4 had a mild, multifocal lymphoplasmacytic and histiocytic myelitis in the thoracic and lumbar segments (Figure 4B).

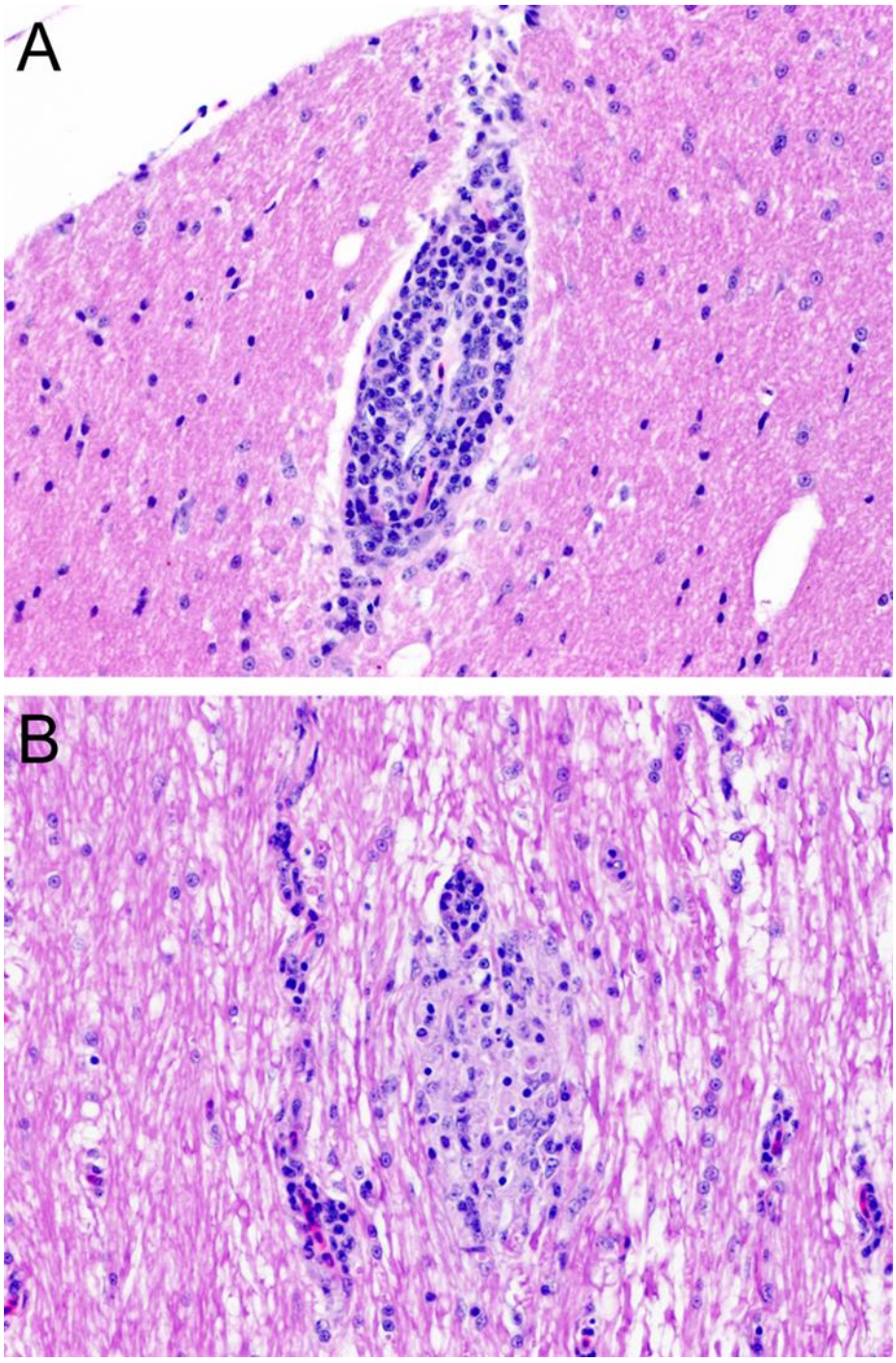

Figure 4. Histopathology. **A.** Chronic, mild, multifocal lymphoplasmacytic encephalitis in quaker parrot 2. **B**. Quaker parrot 4 had a chronic, mild, multifocal lymphoplasmacytic and hystiocytic myelitis.

Discussion

Despite numerous studies published on PDD and its association with PaBV, the pathogenesis of this disease remains unclear. Based on studies in rats inoculated with Borna disease virus (BDV), a T cell-induced immunopathological mechanism has been favored[94] for lesion development in the central and autonomic nervous system of birds inoculated with PaBV; however, few investigators have speculated an autoimmune component might play an important role in PDD pathogenesis.[78, 95] Previous studies developed,[78, 88] suggested that immunization of birds with gangliosides could trigger the development of PDD-like lesions.

In our first study, only one chicken (C1), presented with mild difficulty walking after 14 dpi. The clinical signs were likely related to the inflammatory reaction in the site of inoculation, characterized by a locally extensive granulomatous myositis and steatitis extending to the air sacs. Besides the lesion in the site of inoculation and air sacs, the only histologic lesion seen in this chicken was a lymphocytic infiltrate observed surrounding (but not within) one ganglion and around a vessel of the proventriculus. This lymphocytic infiltrate was interpreted as a lymphoid aggregate, occasionally observed in the gastrointestinal tract of avian species.[96] No histologic lesions were detected in the CNS or PNS of this chicken. Few lymphocytic aggregates were observed in the brain of two chickens, these random infiltrates of mononuclear cells are also occasionally seen in the brain of otherwise healthy chickens.[97]

The clinical signs in quaker parrots were only observed right after the inoculation of gangliosides (mild depression) and were attributed to an expected reaction to the foreign

substances. Histologic lesions were observed in only two quaker parrots and were limited to the CNS. They included a mild, multifocal, lymphoplasmacytic encephalitis (QP2) and a mild, multifocal, lymphoplasmacytic myelitis (QP4). These two quaker parrots also had the highest levels of anti-ganglioside antibodies by ELISA and showed bands compatible with the molecular weight of ganglioside binding proteins on Western blots. Quaker parrot 3 also presented a similar band, but did not have any gross or histologic lesions. All quaker parrots tested negative for PaBV by RT-PCR suggesting that these lesions were provoked by the inoculations rather than a viral agent. We cannot discard the possibility of other nervous components have caused the myelitis in QP4 since this bird was inoculated with non-purified nervous crude extracts. This finding corroborates with the hypothesis that the inoculations might have triggered an autoimmune response, rather than an immunomediated activity, as seen in PDD cases.[17] Most experimental studies involving PaBV inoculation in psittacine birds, were able to induce the first clinical signs of PDD, including depression, regurgitation and undigested seeds in the feces, between 21 and 66 dpi.[17, 32, 36, 98] Additionally, dilation of the proventriculus associated with myenteric ganglioneuritis is a consistent lesion observed in all experimental birds that presented encephalomyelitis and also in most of the natural cases of PDD,[99-101] which supports that if the experimental inoculation of gangliosides is directly related to the development of PDD signs, these classical neurological and gastrointestinal signs and lesions should have been observed during the 83 days of our experiment.

The hallmark of GBS is a peripheral neuropathy with limb weakness, a feature not observed in our experiment (and not a feature of PDD). Although birds unable to walk or

perch have been observed in cases of PDD,[24, 31] inflammatory infiltrates affecting the peripheral nerves responsible for the innervation of the limbs, are not a consistent lesion of PDD.[31, 102] Because encephalomyelitis is one of the common lesions of PDD, a central disorder is more likely to be the cause of impaired deambulation. GBS lesions from nerve biopsies consist of endoneurial and epineurial infiltrates of CD3+ T cells and CD68+ macrophages. Similar lesions are observed in experimental allergic neuritis induced in Lewis' rats, a well-established model of human autoimmune neuropathies (Shin *et al.*, 2013).[103]

Autoreactive T lymphocytes are known to be key players in autoimmune diseases and they can be either regulatory and effector cells.[104] These cells can be activated by several mechanisms including molecular mimicry, and viral and bacterial superantigens.[105] The role of autoreactive T lymphocytes has not been studied in PDD so far, and the importance of T-cell immunopathological mechanisms has only been extrapolated from studies in rats experimentally infected with BDV.[106-108] These studies indicated that the immunopathology of BDV is mediated by $CD8^+$ T cells which require help from $CD4^+$ T cell subsets. These $CD8^+$ T cells have shown active cytolytic activity against target cells infected with BDV or expressing BDV antigens.[109] Macrophages have an essential role in the development of nerve lesions in GBS cases, being associated with axonal demyelination.[28, 110-112] In birds, the lesions caused by PaBV consist of a lymphoplasmacytic infiltrate in either the CNS or PNS[19, 113] and demyelination is not a feature of PDD.

Published studies involving experimental inoculation of PaBV in psittacine birds and following the premises of Koch's postulates[17, 31, 114-116] have been able to induce clinical disease and cause CNS and PNS inflammation in most inoculated birds, supporting the viral etiology of PDD. This data corroborates with the hypothesis that PaBV, like other neurotropic viruses, such as Lyssavirus, directly invades the nervous tissues and triggers inflammation and consequently provokes the damage in the nervous system. Nonetheless, in some diseases such as human idiopathic achalasia, antineuronal antibodies are generated following nervous tissue damage and do not directly influence the development of the disease.[117, 118] A similar association has been proposed for the recent cases of human fatal encephalitis associated with variegated squirrel 1 bornavirus.[25, 119]

In our study, quaker parrots inoculated with gangliosides and examined 83 dpi had no signs of myenteric ganglioneuritis, which differs from experimental studies with PaBV and corroborates with the hypothesis that anti-ganglioside antibodies are not involved in the pathogenesis of PDD. Our results suggest that an autoimmune response to brain gangliosides does not cause the development of PDD-like lesions, and supports that an immune-mediated response might be associated with the pathogenesis of this disease. Additionally, psittacine birds experimentally inoculated with gangliosides and nervous tissues extracts are not an appropriate animal model for GBS. Further studies are needed in order to analyze the participation of anti-gangliosides antibodies in natural cases of PDD and in birds experimentally inoculated with PaBV.

CHAPTER III

PARROT BORNAVIRUS 2 INFECTION PATHOGENESIS IN COCKATIELS (*Nymphicus hollandicus*)[2]

Introduction

Despite the intensive efforts on PDD research, the pathogenesis of this condition and how PaBVs cause disease remain unclear. Several studies were able to reproduce clinical disease and classical lesions of PDD after experimental inoculation of PaBVs and recover this virus in birds that developed the disease, which fulfills Koch's postulates and reaffirms PaBVs as the putative agent of PDD in psittacine birds.[24, 31-33, 36, 120-123] These studies were also able to study the course of avian bornaviruses by analysis of *intra vitam* samples such as swabs and serology. However, they did not evaluate the infection progress and sequence of tissues infected by the virus at different sequential timepoints. The aim of this study was to analyze the infection pathway after experimental inoculation of PaBV-2 in cockatiels using molecular, histological and immunohistochemical methods and to evaluate the viral presence and inflammation at early and later infection.

[2] Reprinted with permission from "From nerves to brain to gastrointestinal tract: A time-based study of parrot bornavirus 2 (PaBV-2) pathogenesis in cockatiels (*Nymphicus hollandicus*)" by Leal de Araujo J, Rech RR, Heatley JJ, Guo J, Giaretta PR, Tizard I, Rodrigues Hoffmann A., 2017. Plos One, 12 (11), e0187797, Copyright 2017 by Leal de Araujo et al.

Material and methods

Ethics Statement

All procedures in this study were conducted using protocols approved by the Texas A&M Biosafety and Animal Use Committees (IACUC 20150-0045) and Institutional Biosafety Committee (IBC2015-021 and IBC2015-142), that meets all federal requirements, as defined in the Animal Welfare act (AWA), the Public Health Service Policy (PHS) and the Humane Care and Use of Laboratory Animals.

Viral culture, titration and inoculum preparation

PaBV-2 isolate was inoculated into duck embryo fibroblasts (DEF, Schubot center laboratory cell collection) cultured for 7 passages in minimum essential medium (MEM) supplemented with 10% fetal bovine serum (FBS, Gibco, ThermoFisher Scientific, Walthan, MA), and subsequently maintained in MEM supplemented with 2% FBS until 70-80% cell confluence. The cells cultures were subjected to three cycles of freeze thaw and brief sonication. The cell debris were removed by centrifugation at 3000g for 10 minutes. Serial 10-fold dilutions of three stocks of virus aliquots were analyzed by focus-forming assays in order to determine viral titration. Titers above 8×10^5 focus forming units per milliliter (FFU/ml) were considered acceptable for the experimental inoculation as previously described.[36, 89]

Experimental animals, virus inoculation, and infection timeline

Thirty-four cockatiels (Nymphicus hollandicus) originated from 2 breeders were used for experimental inoculation of PaBV-2 (CK1-34). Cloacal and choanal swabs from all cockatiels were tested weekly 3 times by RT-PCR in order to exclude the possibility of them being carriers of PaBVs. Twenty-seven cockatiels were inoculated with 0.1 ml of infected DEF lysates containing 8 x 10^4 FFU of PaBV-2 in the right pectoral muscle. Seven cockatiels (CK5, CK8, CK12, CK15, CK20, CK23, and CK32) were inoculated only with 0.1 ml of PaBV-free DEF and served as negative controls. Cockatiels were divided into 12 different groups that corresponded to different euthanasia timepoints (5, 10, 20, 25, 30, 35, 40, 60, 80, 95, 100, and 114 days post-inoculation, dpi) (Fig 1). All cockatiels were evaluated twice a day for any alterations in the normal behavior and general health. Any clinical signs, in special the ones related to PDD (emaciation, anorexia, regurgitation, undigested seeds in the feces and neurological signs) were documented. At the correspondent timepoints or in case the animals presented neurological or/and gastrointestinal signs, cockatiels were humanely and painlessly euthanized with carbon dioxide (CO2) after being anesthetized with isoflurane (IsoThesia, Henry Schein, Melville, NY). Cockatiels were kept in cages with no more than 6 animals, with access to high-quality food, water, solar light and environmental enrichment. Animals with clinical signs of diseases other than PDD were excluded from the experiment and treated accordingly. One cockatiel originally obtained for this study had a self-inflicted traumatic injury and it was excluded from the experiment.

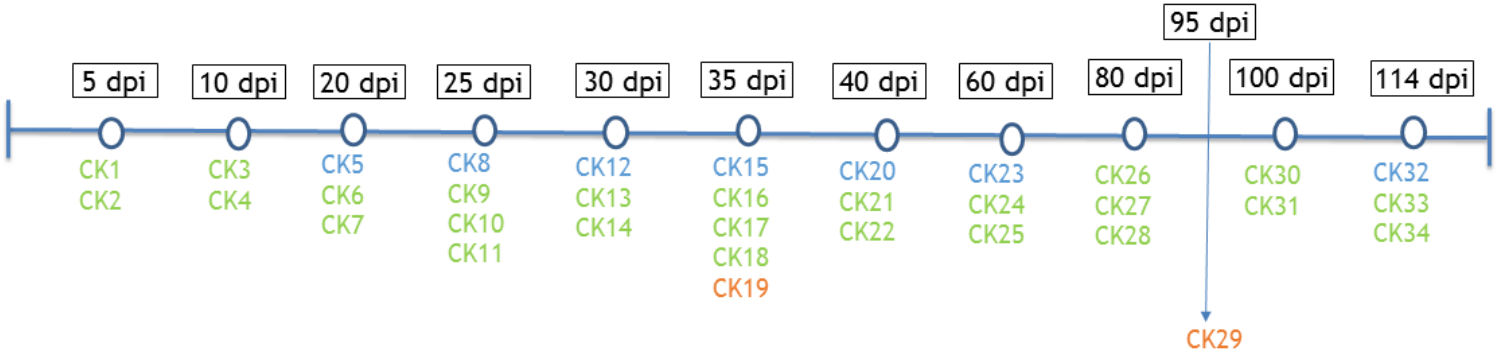

Figure 5 Distribution of infected (green) and control (blue) cockatiels throughout timepoints. Cockatiels that naturally died during the experiment are represented in orange.

Postmortem examination and sample collections

A complete necropsy was performed in each bird. During necropsies, samples from cloacal and choanal swabs, blood, site of inoculation (pectoral muscle), feather calamus, skin between the scapulae, skin from wing, skin behind the neck, crop, proventriculus, ventriculus, small intestine, large intestine, kidney, spleen, heart, liver, brain, spinal cord, brachial plexus and adrenal gland were collected for RT-PCR. Additionally, samples from skin behind the neck, skin between the scapulae, skin from the wing, skin from uropygium, site of inoculation (pectoral muscle), leg muscle, brachial plexus, vagus nerve, sciatic nerve, heart, thyroid and parathyroid glands, tongue, pharynx/larynx, thymus, esophagus, crop, proventriculus, ventriculus, small intestine, pancreas, large intestine, cloaca, spleen, liver, kidney, adrenal glands, trachea, syrinx, lungs, brain, spinal cord, eyes, head sinuses, tibiotarsus, and adjacent ganglia of all organs were also collected for histopathology and immunohistochemistry.

Histopathology and immunohistochemistry

Samples collected during necropsy were fixed in 10% neutral buffered formalin and processed routinely for histopathology. A morphologic diagnosis indicating chronicity, severity, and nature of lesions was documented for each organ or tissue. Lymphoplasmacytic inflammation related to PaBV-2 infection was scored as follows: - (absent), + (minimal), ++ (mild), +++ (moderate), ++++ (severe). Immunohistochemistry was performed on the serial tissue sections, mounted on charged slides, and examined by light microscopy. Processing was done on an automated stain equipment, using rabbit

polyclonal antiserum raised against PaBV-2 N protein. Briefly, after manual deparaffinization and rehydration, antigen retrieval was performed on a pressure cooker utilizing the commercial compound EMS buffer C, PH 4.5 (Electron microscopy sciences, Hatfield, PA) for 20 min under 121°C. Sections were treated with 0.3% hydrogen peroxide in order to block endogenous peroxidase activity for 45 minutes and with a protein blocker for endogenous protein activity for 10 minutes. Slides were incubated with rabbit anti-PaBV-N serum (1:1000) for 1 hour, followed by 10 minutes incubation with antibody enhancer and 15 minutes incubation with a goat anti-mouse/rabbit polymer visualization system (Thermo Fisher Scientific, Waltham, MA). Additionally, 3, 3'-Diaminobenzidine (DAB, Thermo Fisher Scientific) was used as a chromogen for color development. Slides were counter-stained with hematoxylin and examined under light microscopy. Polyclonal antibodies were developed by a commercial company (Lifetein, Somerset, NJ) against a specific region of the PaBV-2 N-protein. Due to the intranuclear replication nature of PaBVs, only cells with intranuclear or intranuclear and intracytoplasmic immunolabeling were considered positive. Cells only with intracytoplasmic immunolabeling were considered negative. Slides were scored based on the amount of positive cells in the section: - (absent), + (1-3% affected cells), ++ (4-10% affected cells), +++ (11-25% affected cells) and ++++ (more than 25% affected cells). The score of histopathology and immunohistochemistry for each timepoint was based on the average of the results of all birds in the respective timepoint. However, when only one bird presented inflammation or was positive by IHC, its score was considered representative for the timepoint. A

complete list of results for each individual bird is available as supporting information (Supporting table 1).

RNA extraction, RT-PCR and agarose gel electrophoresis

Collected samples were evaluated for presence of PaBV-2 RNA by RT-PCR detection of PaBV-2 matrix (PaBV-M) genes, as previously described.[124] Viral RNA was extracted from tissues using an RNeasy mini kit (Qiagen, Valencia, CA, USA), following manufacturer's instructions. Viral RNA was reverse transcribed using high capacity cDNA synthesis kit (Applied Biosystems, Foster City, CA) and cDNA generated using random primers. Finally, PaBV-2 cDNA was amplified using the following primers targeting the M (Matrix) protein gene: PaBV M F (5-GGTAATTGTTCCTGGATGG-3) and PaBV M R (5-ACACCAATGTTCCGAAGACG-3). The PaBV-2-infected DEF used for viral culture were used as a positive control. After amplification, the PCR products were separated by size using electrophoresis in an agarose gel that was examined under ultraviolet light. Bands on the agarose gel were scored as positive (+) or negative (-). The timepoint was considered positive for PaBV-2 RNA by RT-PCR when at least one bird was positive in the given timepoint. Selected samples were also tested by qPCR as previously described elsewhere,[124] and using primers and probes targeting the M protein gene: ABV M1F primer-5-GGTAATTGTTCCTGGATGG-3 (36 μM) and ABV M2R primer-5-GG[Y]TC[Y] [Y]TCACTGAAAGAAA[H]GG-3 (36 μM), and ABV M TaqMan Probe -5 FAM-CCAACAAAGTCTAT[Y]TCCA[R]C-3 -BHQ (10 μM), in order to compare sensitivity and confirm the conventional PCR results. Quantification cycles

above 35 were considered negative, based on our standard curve threshold. A complete list of RT-PCR and qPCR results for each individual bird is available as supporting information (Supporting table 2).

Results

Clinical disease and macroscopic findings

At 35 dpi, one of the cockatiels (CK19) presented with acute signs of depression, dyspnea, and lethargy (Fig 2A), and died shortly thereafter. A post-mortem examination was promptly performed. At 60 dpi, CK24 presented with mild signs of lethargy, ruffled feathers and regurgitation (Fig 2B) and euthanasia was elected, followed by necropsy. Additionally, CK29 was found dead at 95 dpi with no prior signs of illness. Macroscopic lesions were observed in 6 cockatiels (CK19, 23, 28, 29, 33, 34) and consisted of crop and/or proventricular dilatation (Fig 3B). None of the control birds presented clinical signs or macroscopic lesions.

Figure 6 Clinical signs of cockatiels (*Nymphicus hollandicus*) infected with PaBV-2. Lethargy and depression of CK19 at 35 dpi (A) and ingesta-stained feathers in the foreneck and breast of CK24 (60 dpi) after regurgitation (B).

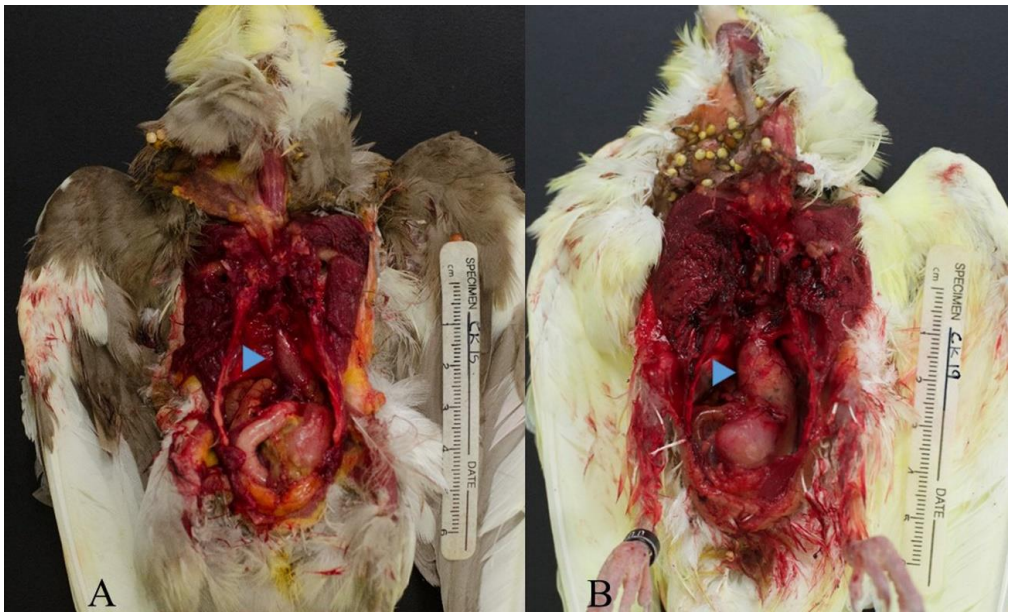

Figure 7 Gross findings. Comparison of proventriculus size (arrowheads) in a control (A) and infected (B) cockatiels of the same timepoint (35 dpi). Note the distention of the proventricular wall in CK19 when compared to a control cockatiel (CK15).

Microscopic findings

Inflammatory lesions were observed as soon as 5 dpi in the site of inoculation, which was a consistent finding throughout all timepoints and most likely to be caused by the injection itself. This inflammatory infiltrate was characterized by multifocal aggregates of lymphocytes, plasma cells and macrophages and ranged from a minimal to severe myositis frequently organized around vessels, and extending to intercostal and pectoral nerves. The first lesions outside the site of inoculation were then observed in the brachial plexus at 20 dpi in CK6 and consisted of minimal lymphoplasmacytic neuritis. At 25 dpi, inflammatory lesions were observed in the cervical, thoracic and lumbar segments of the spinal cord and adjacent ganglia, as well as in the brain. Inflammation in the CNS was comprised of perivascular cuffing, mainly in the gray matter and meninges, with occasional gliosis and glial nodules at later timepoints. From 25 dpi and beyond, encephalitis and/or myelitis were consistently observed in all cockatiels. At 30 dpi, besides the CNS, inflammatory lesions were observed in the crop and intestinal ganglia, vagus nerve and in the adrenal medulla and adjacent ganglia. CK19, at 35 dpi, was not only the first cockatiel to develop clinical signs of PDD and die, but also the first cockatiel to present proventricular and ventricular ganglioneuritis and also lymphoplasmacytic infiltrates in the optic and sciatic nerves. These lesions were intermittently observed in the subsequent timepoints. At 40 dpi, the epicardial and renal ganglia, and nerves in the cloacal region presented the first inflammatory lesions. A lymphoplasmacytic dermal neuritis was observed at 80 dpi, and the skin from the wing was not only the first skin site to present inflammation but the most frequent one, being further observed at 95, 100, and

114 dpi. Dermal neuritis was observed in the skin from the uropygial gland (95, 100, and 114 dpi), skin behind the neck (80, 100, and 114 dpi) and skin between the scapulae (100 and 114 dpi). These histopathological findings were observed intermittently until 114 dpi and severity ranged from minimal to severe. No lesions related to PaBV-2 infection were observed in the liver, spleen, tongue, leg muscle, trachea, lungs, head sinuses, syrinx, thyroid and parathyroid glands, tibiotarsus, or thymus of any infected cockatiels. Additionally, no inflammatory lesions associated with bornavirus infection were observed in any tissues of the control cockatiels.

Immunohistochemistry

The site of inoculation was consistently positive throughout the timepoints, with lower signal with the progression of the infection and no signal at the last two timepoints. Lymphocytes and plasma cells presented positive intranuclear immunolabeling and macrophages presented intracytoplasmic labelling in these sites (Fig 4B). Nuclei of Schwann cells in the branches of the intercostal and pectoral nerves were also positive in some of the early timepoints (Fig 4B). Brachial plexus was the first site outside of the pectoral muscle to demonstrate intranuclear immunolabeling in Schwann cells starting at 20 dpi. Neurons of the dorsal root ganglia had a similar immunolabeling at this timepoint (Fig 4F). Neurons of the ventral horn in the thoracic segment of the spinal cord were the first cells in the CNS to present positive intranuclear and intracytoplasmic immunolabeling at 20 dpi. After 25 dpi, neurons and glial cells in the cervical and lumbar segments of the spinal cord as well as throughout the brain presented intranuclear and intracytoplasmic immunolabeling (Fig 4J). These sites were consistently positive until the end of the experiment, varying in severity and extension. Simultaneously at 30 dpi, neurons of the ingluvial and intestinal ganglia were the first immunolabeled cells in the gastrointestinal tract along with adrenal ganglia neurons and cells of the adrenal medulla (Fig 4R) were positive. Ganglia and nerves of the proventriculus (Fig 4N), ventriculus, and eyes as well as the vagus nerve were first positive at 35 dpi. Esophageal, epicardial, renal and cloacal ganglia were first positive at 40 dpi. At 60 dpi, scattered cells of islets of Langerhans of the pancreas were positive, which were intermittently positive until 114 dpi. Interestingly, at 80 dpi, nerves and the smooth muscle in the skin (Fig 4X) from

multiple regions (behind the neck, wing and uropygial gland) and also the smooth muscle of crop, proventriculus, ventriculus, intestines, cloaca and tunica media of vessels from different tissues, including the spleen, started to have a diffuse immunolabeling that was intermittently positive until the last timepoint. Epithelial cells of the GI system also showed few scattered intranuclear immunolabeling at this timepoint. Additionally, nerves and smooth muscle of the feathered skin between the scapulae and the squamous epithelium and occasionally the feather shaft of feather follicles from the wing started to be positive at 100 dpi and 114 dpi, respectively. Samples from tongue, trachea, lungs, head sinuses, syrinx, thyroid, parathyroid, tibiotarsus, or thymus, were negative at all timepoints and no control cockatiels presented immunolabeling in any of the examined tissues.

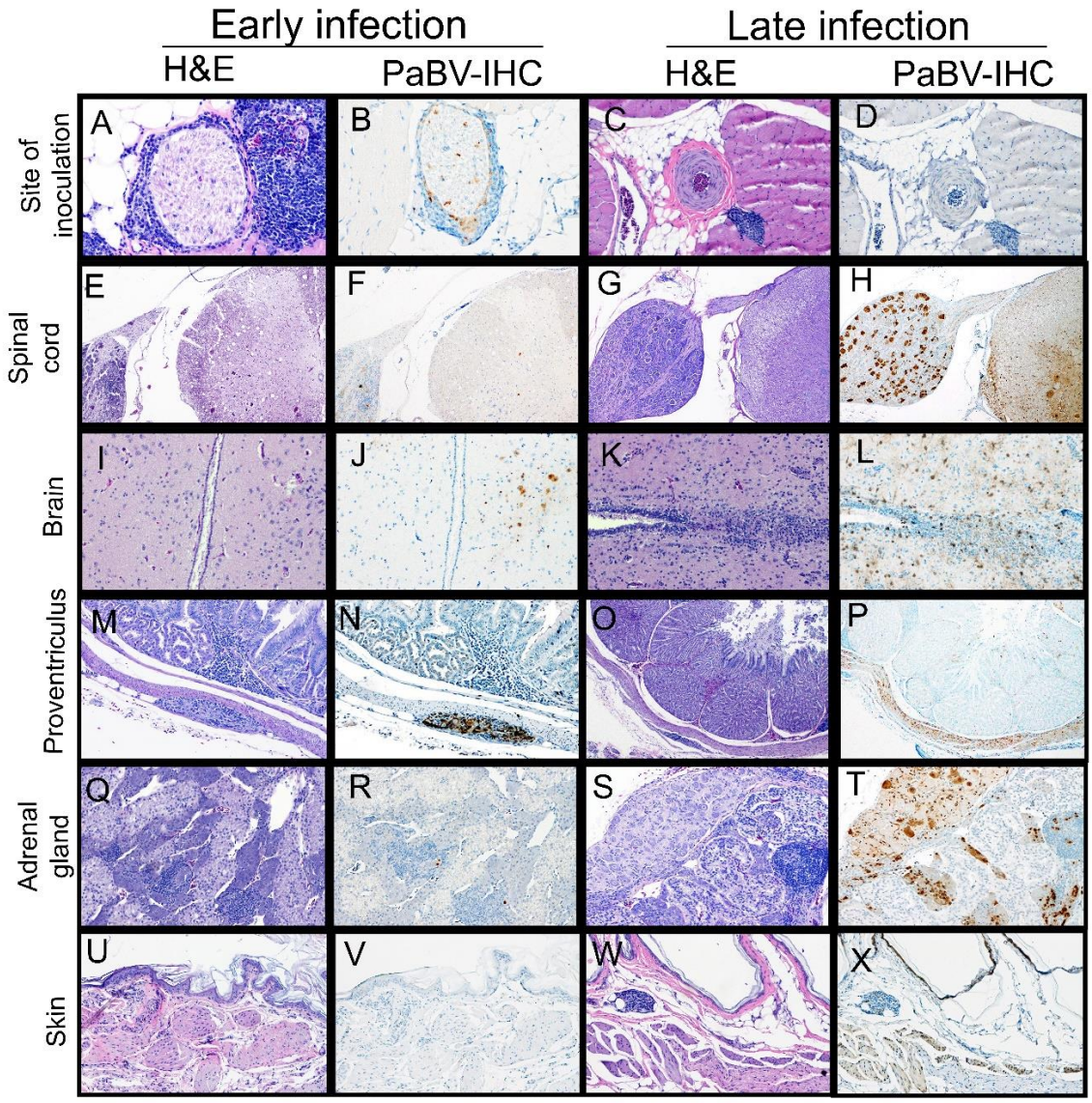

Figure 8 Sequence of histological findings and immunohistochemical labelling in tissues from infected cockatiels during early and late infection. The first tissue to present lymphoplasmacytic inflammation and positive labelling was the site of inoculation, which showed marked lymphoplasmacytic myositis (A) and positive immunolabeling in the nuclei of inflammatory cells as well as in Schwann cells of intercostal and pectoral nerves (B) in early infection (CK2, 5 dpi) and reduced inflammatory infiltrates (C) and no positive immunolabeling (D) at late infection (CK34, 114 dpi). PaBV then reached the spinal cord through adjacent ganglia and nerves, which provoked minimal myelitis (E) and infection of few neurons (F) in the early timepoints (CK9, 25 dpi) and severe inflammation (G) and widespread viral distribution (H) in late infection (CK26, 80 dpi). When PaBV reached the brain (CK10,

25 dpi), minimal inflammation (I) and positive immunolabeling of few neurons (J) was observed, whereas severe inflammation (K) accompanied by widespread immunolabeling (L) was observed in chronically infected cockatiels (CK30, 100 dpi). Only after invasion of the CNS, PaBV was identified at 30 dpi (CK19) in the GI tract (N), initially with mild inflammation (M) that progressed to moderate to severe ganglioneuritis (O) and diffuse immunolabeling in ganglia, smooth muscle and few scattered epithelial cells (P) in the late infection timepoints (CK28, 80 dpi). Adrenalitis was only observed in small areas of the adrenal medulla (Q) accompanied by scattered PaBV positive cells (R) in the early infection (CK14, 30 dpi), however, adrenalitis and ganglioneuritis (S) were severe in late infection (CK25, 60 dpi) and followed by wide spread immunoimmunolabeling (T) affecting the adrenal medulla and adjacent ganglia. Finally, tissues such as skin had no inflammation (U) or immunolabeling (V) in the early infection timepoints (CK7, 20 dpi) but presented multifocal positive immunolabeling pattern (X) in late infection (CK34, 114 dpi), accompanied by mild to moderate inflammation (W).

RT-PCR

All samples from the site of inoculation for the timepoints between 20 and 114 dpi were positive for PaBV RNA by PCR. The brachial plexus, spinal cord, brain, crop, proventriculus, ventriculus, small intestine, large intestine, adrenal gland and heart/great vessels of the heart RT-PCR results were positive and correlated to the IHC positive results. Cloacal swabs were first positive at 35 dpi and choanal swabs at 60 dpi, and both samples remained positive until 114 dpi. Although the feathered skin between the scapulae was negative by IHC until 95 dpi and the skin behind the neck and from the wing were negative until 80 dpi, these samples were positive by RT-PCR as early as 60 dpi. Samples from spleen were positive at 100 and 114 dpi. Samples from blood and liver were collected and tested by RT-PCR but were negative at all timepoints. Unfortunately, samples from the site of inoculation were not available at 5 and 10 dpi. All samples from control cockatiels were negative at all timepoints.

Real time PCR was one serial dilution more sensitive than conventional PCR when 10-fold dilutions were compared between the 2 techniques, therefore selected samples from cloacal and choanal swabs, brachial plexus, spinal cord and brain for early time points, and samples from blood and liver of all cockatiels were tested with this more sensitive technique in order to confirm the accuracy of conventional PCR results. For the early time points, samples of cloacal and choanal swabs, brachial plexus and spinal cord tested positive in additional cockatiels that were negative by conventional PCR. However, these cockatiels were within timepoints where other birds were already positive by conventional PCR. One exception was the choanal swab, which was positive in one cockatiel (CK22)

at 40 dpi, while conventional PCR first detected it at 60 dpi. Viral RNA was only detected in samples of spleen from cockatiels that were positive by conventional PCR. All samples of liver and blood tested negative at all time points. A complete list of the qPCR results can be found as supporting information (supporting table 2).

Discussion

This is the first experimental study to demonstrate the viral spread and distribution of histological lesions in a time-based approach after intramuscular inoculation of PaBV-2 in cockatiels (Fig 5). PaBV-2 was first detected in the areas of inflammation in the site of inoculation in the pectoral muscle, reaching branches of the intercostal and pectoral nerves. Subsequently, PaBV-2 reached the brachial plexus, and centripetally extended through the dorsal root ganglia to the spinal cord, which was followed by the invasion of the brain. After successfully invading the CNS, PaBV-2 centrifugally spread to the ganglia in the gastrointestinal system, adrenal gland, heart and kidneys through the sympathetic and/or parasympathetic innervation. Finally, a shift in the specific tropism of the virus was observed in the late timepoints, and not only nerves and ganglia were affected but also the smooth muscle and/or scattered epithelial cells of tissues such as crop, intestines, proventriculus, kidneys, skin, and the tunica media of the vessels culminating in a widespread viral distribution.

Previous experimental studies with PaBV-2 and PaBV-4 have been able to successfully induce clinical disease, and the classical meningoencencephalomyelitis and ganglioneuritis. [31, 32, 37, 114, 120-123] However, whether the virus spread to the CNS from the

PNS or vice-versa was never clearly understood since in these studies the birds were only euthanized when they presented clinical disease or at the end of the experiment. Therefore, these investigations analyzed early infection aspects only by intra vitam parameters such as viral shedding and seroconversion, and important information about the viral pathway that was present in the early infection, and could have been detected by histopathology and immunohistochemistry, was consequently missed. Interestingly, we first detected viral RNA in cloacal swabs at 35 dpi and in choanal swabs at 60 dpi, which contrasts with some experimental studies in canaries and cockatiels where viral shedding was detected intermittently after the first week post-inoculation.[123, 125] However, important factors such as the species used in the experiment and mixed routes of experimental infection must be taken into consideration for explaining this earlier viral shedding. Additionally, other studies using intramuscular and subcutaneous route of infection in cockatiels were able to first detect viral RNA in swabs between 7 and 11 weeks post-inoculation, which corroborates with our results.[122]

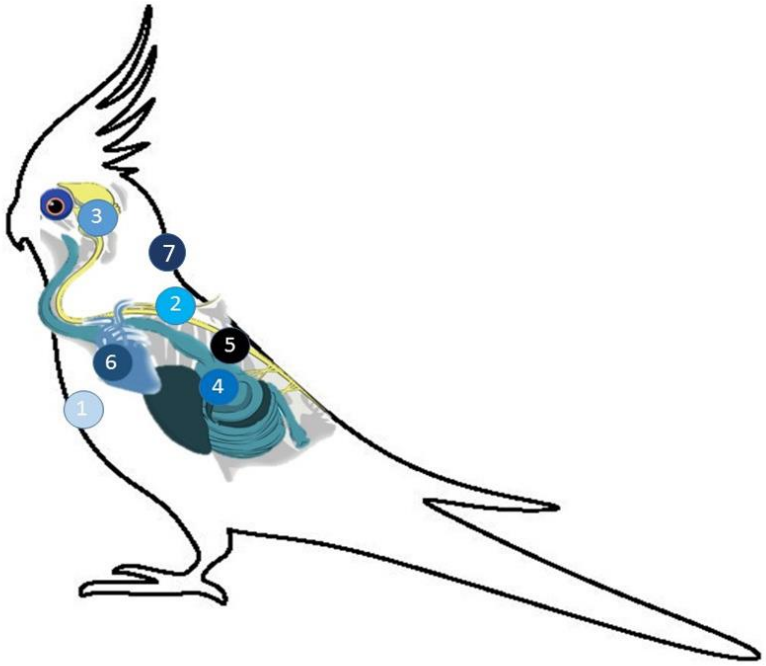

Figure 9 Chronologic infection pathway based on PaBV N-protein detection by IHC. Positive immunolabeling after intramuscular inoculation (1) was first observed at 20 dpi in the spinal cord (2), followed by brain (3) at 25 dpi. Ganglia in the GI tract (4) and adrenal gland (5) were first positive at 30 dpi. Positive immunolabeling in the epicardial ganglia (6) was first observed at 35 dpi. Extra-neural tissues such as skin (7) only had positive immunolabeling at late infection timepoints, as early as 80 dpi.

The natural route of infection of PaBVs is a nebulous aspect of PDD pathogenesis. Experimental studies were able to infect psittacine birds using single intramuscular, intravenous or intracerebral routes[32, 35, 120] or using different protocols of intramuscular, oral, oculonasal, and subcutaneous routes combined.[21, 31, 37, 114] Recently, two studies involving cockatiels inoculated by oculonasal or oral routes failed to establish persistent PaBV-2 or PaBV-4 infection or to induce PDD lesions in any of the birds during 6 months of experiment[65] suggesting that these routes are unlikely to be involved in natural PaBV-2 infection. Furthermore, in our experiment, the successful induction of PaBV-2 infection through intramuscular inoculation, and the widespread distribution of PaBV-2 in late infection timepoints indicate that direct transmission of PaBV-2 through trauma wounds or tegument injury might play a pivotal role in the pathogenesis. A novel bornavirus recently identified in variegated squirrels (Variegated squirrel bornavirus-1; VSBV-1) was linked to three cases of fatal encephalitis in humans who were breeders of this squirrel species.[25] Although the route of infection still remains unclear in these cases, family members reported skin injuries due to squirrel bites and scratches for 2 of the patients, which indicates that this route of infection might be involved in the VSBV-1 transmission. Interestingly, VSBV-1 RNA was observed in several tissues of the variegated squirrels that had contact with the breeders, including brain, heart and kidneys, and VSBV-1 RNA and antigen were identified in the neurons, glial cells and neuropil in the brains of the breeders. The hypothesis that VSBV-1 could be transmitted via skin injuries is further supported by a recent study where 11 out of 468 squirrels originated from private institutions, zoological gardens and roadkill were screened in Germany and Netherlands

and tested positive for VSBV-1 RNA with the highest loads in the CNS, oral cavity and skin.[126] Furthermore, the presence of VSBV-1 in the oral cavity of infected variegated squirrels could be associated with transmission of this virus to humans in eventual biting accidents.

Neurotropic pathogens can invade the brain by different strategies, including retrograde axonal transport, hematogenous spread across the blood-brain barrier (BBB), direct infection of endothelial cells and via spread of infected leukocytes across the BBB into the parenchyma, also known as "trojan horse" mechanism.[127] In the early timepoints of our experiment, PaBV-2 was restricted to branches of pectoral muscle nerves, brachial plexus, neurons of the dorsal root ganglia and spinal cord, even before inflammation could be observed in the latter two tissues. Only after reaching the brain, PaBV-2 was observed spreading to extra-neural tissues. Our results suggest that PaBV-2 reaches the CNS through retrograde axonal transport in a similar way to another neurotropic negative sense single-stranded RNA virus such as Rabies virus (RABV). RABV is transmitted by the bite of infected animals, infects motor neurons at the neuromuscular junctions in the site of injury, and then spreads to the spinal cord by retrograde axonal transport, which eventually leads to infection of the brainstem and limbic system.[128] Once in the brain, RABV migrates throughout the CNS and then back to the periphery via anterograde axonal transport. Late in infection, the virus can be seen in the skin, salivary glands, heart, kidney and cornea.[129] Experimental studies have provided evidence that Borna disease virus 1 (BoDV-1) uses nerve endings in the nasal and pharyngeal mucosa to gain access to the olfactory bulb and consequently to the brain via retrograde axonal transport and can infect neurons,

astrocytes, ependymal cells and oligodendrocytes of experimentally infected rodents.[130] In contrast to the scenario seen in PaBV reservoir hosts, mammalian Bornaviruses are strictly neurotropic and encephalitis is the most striking manifestation of bornaviral infection in its dead-end hosts, including horses, sheep, cats, and rodents.[129] In contrast, in the bicolored shrew (Crocidura leucodon), the natural reservoir of BoDV-1, this Bornavirus was identified in several neural and extra-neural tissues, and continuously shed through secretions, excretions, and even skin scalping.[131] BoDV-1 infection in experimental and erroneous hosts is mainly restricted to the gray matter of the brain and spinal cord, and despite vision impairment has been mostly attributed to central blindness,[130] degeneration of retinal neurons has also been reported.[132] Other neurotropic agents such as Poliovirus[133] or Scrapie prions[134] may also use retrograde axonal transport to spread to the CNS, however, in these cases, viremia and/or infection of the gastrointestinal associated lymphoid tissue (GALT) occur after oral ingestion of these agents, which precedes invasion of CNS.

The combination of immunohistochemistry and molecular methods used in our experiment was able to provide valuable information about viral antigen localization and its relationship with viral RNA. For instance, although samples from spleen were positive by PCR at 100 and 114 dpi, IHC revealed that only smooth muscle of the splenic vessels were positive, which corroborates with the late infection pattern seen in our study and agrees with the results of other studies that were able to demonstrate only low viral loads in this tissue.[32, 122] Additionally, we could not detect viral antigen nor viral RNA in any

samples of liver, which also corroborates with other studies that demonstrate very low or no load of PaBV-2 in this tissue.[122, 123]

Although a slow growing virus in cell culture, PaBV-2 detection can be observed in vivo as early as 20 dpi, using an intramuscular route of infection. Interestingly, despite the hallmark lesion of PaBV infections being the dilation of the proventriculus, our results demonstrated this virus affects the CNS at least 10 days before migrating to peripheral tissues like the GI system. In the late infection, viral tropism for neural tissue is not as strict as in the early infection timepoints, and PaBV-2 has broad tissue tropism affecting extra-neural tissues. Our findings reinforce the potential of samples for antemortem diagnostic methods such as crop immunohistochemistry and cloacal swabs PCR for detection of PaBV-2 in early infection timepoints, as early as 30 and 35 dpi, respectively. Additionally, skin samples and choanal swabs might be useful for detection of PaBV-2 by RT-PCR in chronically infected patients. On the other hand, we were not able to detect PaBV-2 RNA in the blood of any of the cockatiels in this experiment, which corroborates with other studies that concluded that blood samples are not reliable for PaBV-2 detection by RT-PCR[30, 66, 135] and viremia is unlikely to take place in the pathogenesis of PDD. Future research is necessary to understand key features of PaBV-2 infection and PDD pathogenesis such as natural route of infection, receptors in target cells, and immune response.

CHAPTER IV

DISTRIBUTION OF INFLAMMATORY LESIONS AND VIRAL ANTIGEN IN COCKATIELS (*Nymphicus hollandicus*) EXPERIMENTALLY INFECTED WITH PARROT BORNAVIRUS 2

Introduction

Neurotropism is an important feature of mammalian bornaviruses and has been extensively studied in natural and experimental cases of Borna disease.[43, 94, 129, 136] BoDV-1 infection occurs in horses and sheep in central Europe[137] and causes a lymphoplasmacytic meningoencephalomyelitis with predilection for the gray matter. It affects primarily the hippocampus, caudate nucleus, substantia nigra, mesencephalon and hypothalamus.[4, 13] Eosinophilic intranuclear inclusion bodies known as Joest-Degen bodies are produced by the viral replication machinery[138] and, although not a consistent finding, they can be seen in neurons of animals affected by Borna disease,[139] and are particularly prominent in the hippocampus.[140] Additionally, retinal degeneration and lymphoplasmacytic optic neuritis have been reported as a cause of blindness in horses infected with BoDV-1.[132, 141] BoDV-2 was isolated from a horse with severe neurological disease in Austria and although it differs from BoDV-1 by more than 15% of nucleotide identity, the clinical and pathological presentation were identical to BoDV-1 infections.[142]

The distribution of inflammatory lesions of natural and experimental bornaviral diseases in other mammals such as variegated squirrels, humans and immunocompetent rodents are similar to those observed in horses and sheep.[4, 40] In contrast, neonatal rodents

experimentally inoculated with BoDV-1 lack evidence of encephalitis, but suffer significant developmental injury in the central nervous system (CNS), particularly in the hippocampus and cerebellum including dentate gyrus involution and the loss of cerebellar granular cells, respectively.[13, 136, 143]

Neurons, glial and ependymal cells are the main target cells of the brains infected by both mammalian and avian bornaviruses.[144-148] Immunolabeling is expressed in the nuclei alone or nuclei and cytoplasm of these cells, reflection of the intranuclear replication of the bornaviruses,[21] a characteristic shared among only three other taxa of animal RNA viruses: the families Orthomyxoviridae, Retroviridae and Nyamiviridae.[13-15]

Although neurotropism is a prominent characteristic of PaBVs, studies on the precise localization of inflammatory lesions and viral distribution are limited and lack a systematic approach.[149, 150] The aim of this study was to analyze the distribution of inflammatory lesions and PaBV nucleoprotein antigen localization in a chronologic and systematic manner to ultimately provide a good understanding of the CNS areas affected by this virus and its pathogenesis.

Material and methods

Ethics Statement

All procedures in this study were conducted using protocols approved by the Texas A&M Biosafety and Animal Use Committees (IACUC 20150-0045) and Institutional Biosafety Committee (IBC2015-021 and IBC2015-142), that meets all federal

requirements, as defined in the Animal Welfare act (AWA), the Public Health Service Policy (PHS) and the Humane Care and Use of Laboratory Animals.

Viral culture and inoculum preparation

Parrot bornavirus 2 (PaBV-2) was inoculated into duck embryo fibroblasts (DEF, Schubot Exotic Birds health center laboratory cell collection) cultured in minimum essential medium (MEM) supplemented with 10% fetal bovine serum (FBS, Gibco, ThermoFisher Scientific, Walthan, MA), and subsequently maintained in MEM supplemented with 2% FBS, as previously described.14

Experimental animals, virus inoculation, and infection timeline

Thirty four cockatiels (Nymphicus hollandicus) originated from two PaBV-negative aviaries were used for experimental inoculations of PaBV-2 (CK1-34), as previously described.27 Briefly, cockatiels were divided into 12 different groups that corresponded to different euthanasia timepoints (5, 10, 20, 25, 30, 35, 40, 60, 80, 95, 100, and 114 days post-inoculation, dpi). Twenty-seven cockatiels were inoculated with PaBV-2 while seven cockatiels were inoculated only with PaBV-free DEF and served as negative controls. Cockatiels were inoculated using intramuscular injection in the right pectoral muscle with 4x104 focus-forming units of virus. Any clinical signs observed during the experimental period were documented. At the correspondent timepoints, cockatiels were anesthetized with isoflurane (IsoThesia, Henry Schein, Melville, NY) and then humanely euthanized with carbon dioxide (CO2).

Histology

Brain and spinal cord of each bird were placed in 4% neutral formaldehyde for 48 hours. Coronal sections of the brain were obtained from the cerebrum at the level of the hyperpalium and nucleus basorostralis (Level I), cerebrum at the level of the striatum (Level II), and cerebrum at the level of the arcopalium and hindbrain (Level III). Additionally, a sagittal section was taken from the rhombencephalon encompassing the hindbrain, midbrain and cerebellum (Level IV) (Figure 1).

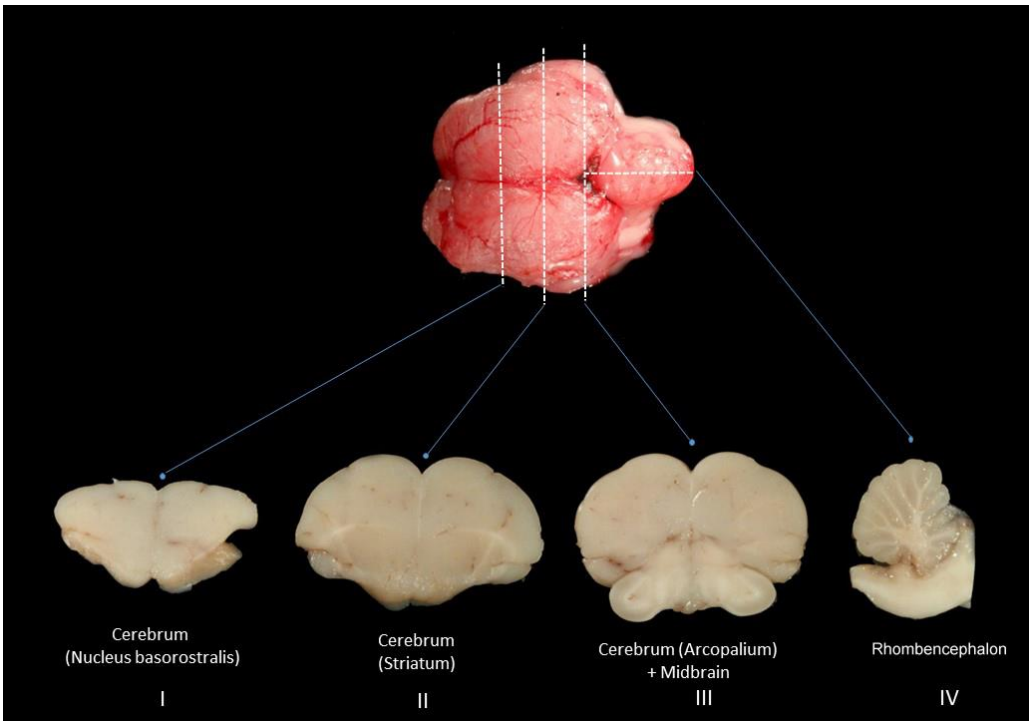

Figure 10. Selected levels of the brain for histological and immunohistochemical analysis in PABV-2 inoculated cockatiels. I. Cerebrum at the level of the nucleus basorostralis. II. Cerebrum at the level of the striatum. III. Cerebrum at the level of the arcopalium and midbrain. IV. Brain at the level of the rhombencephalon, encompassing cerebellum and brainstem.

Four transversal serial samples from cervical spinal cord between C1 and C13, thoracic spinal cord between T1 and T7 and the lumbosacral spinal cord at the level of the fused vertebrae of the synsacrum and the 5 caudal vertebrae (Figure 11) were also collected from all birds. Samples of spinal cord were collected with intact vertebrae and submitted to decalcification, which allowed the visualization of the adjacent spinal ganglia. All samples were processed routinely for histologic examination.

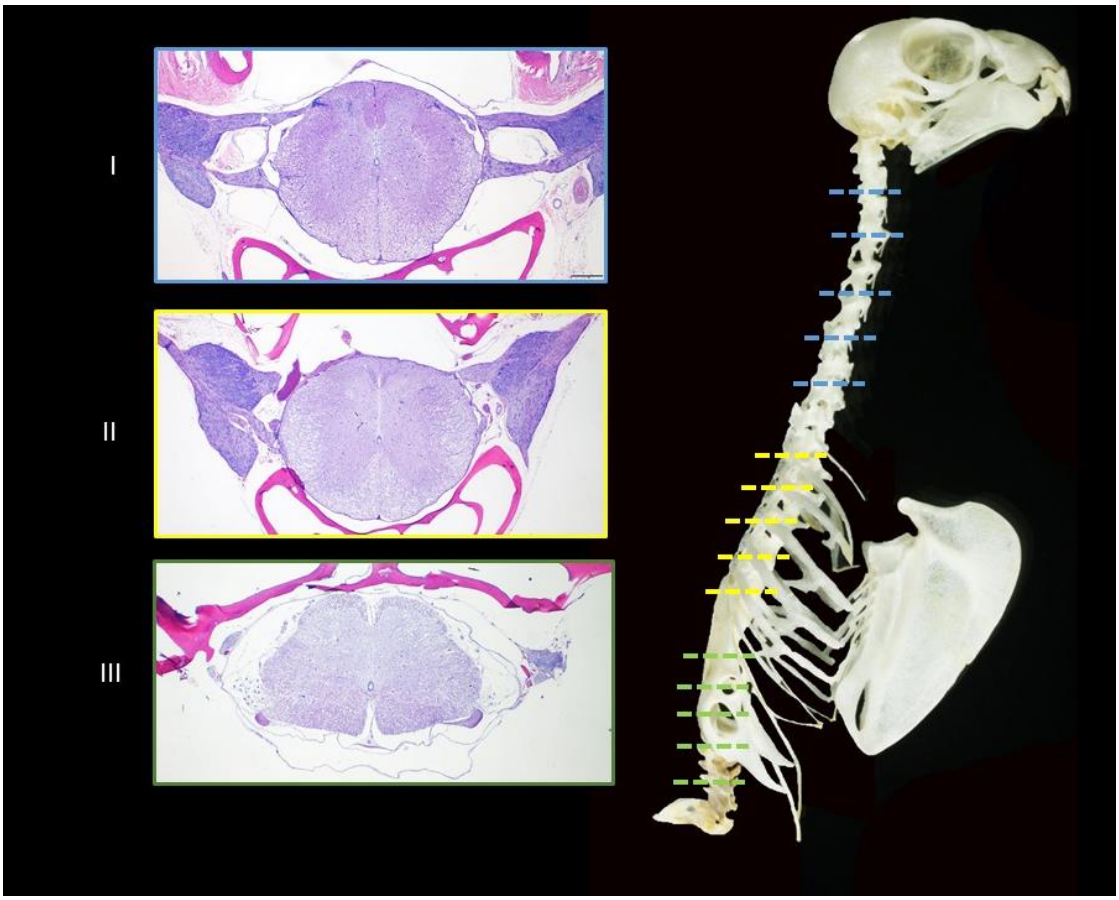

Figure 11. Selected levels of the spinal cord for histological and immunohistochemical analysis of lesion in PaBV-2 inoculated cockatiels. I. Cervical spinal cord (C1-C13). II. Thoracic spinal cord (T1-T7). III. Lumbosacral spinal cord (Synsacrum and S1-S5).

The neuroanatomic location of each inflammatory focus was mapped in a diagram and the description of the regions of the brain followed what has been suggested by the avian brain nomenclature consortium,[151-153] and adapted for this purpose (Figure 3). A single vessel surrounded by layers of lymphocytes and plasma cells or a glial nodule was interpreted as a single inflammatory focus and was indicated by a dot in the diagram. The severity of inflammation was represented by four different dot sizes (minimal, mild, moderate or severe) and each bird with inflammatory lesions was represented by a different color. Lesions were considered minimal when one single layer of perivascular cuffing and no more than one focus was in the analyzed section; mild when two layers of inflammatory cells and/or between two to three foci were in the analyzed section; moderate when vessels had by three layers perivascular cuffing and/or between four to seven foci in the analyzed section and severe when four or more layers of perivascular cuffing and/or more than six inflammatory were foci in the analyzed section. All sections were analyzed separately for each bird and then overlapped to generate the final diagram using a graphic software (Photoshop elements, Adobe systems, San Jose, CA). Lymphoplasmacytic inflammation related to PaBV-2 infection was scored as follows: - (absent), + (minimal), ++ (mild), +++ (moderate), ++++ (severe).

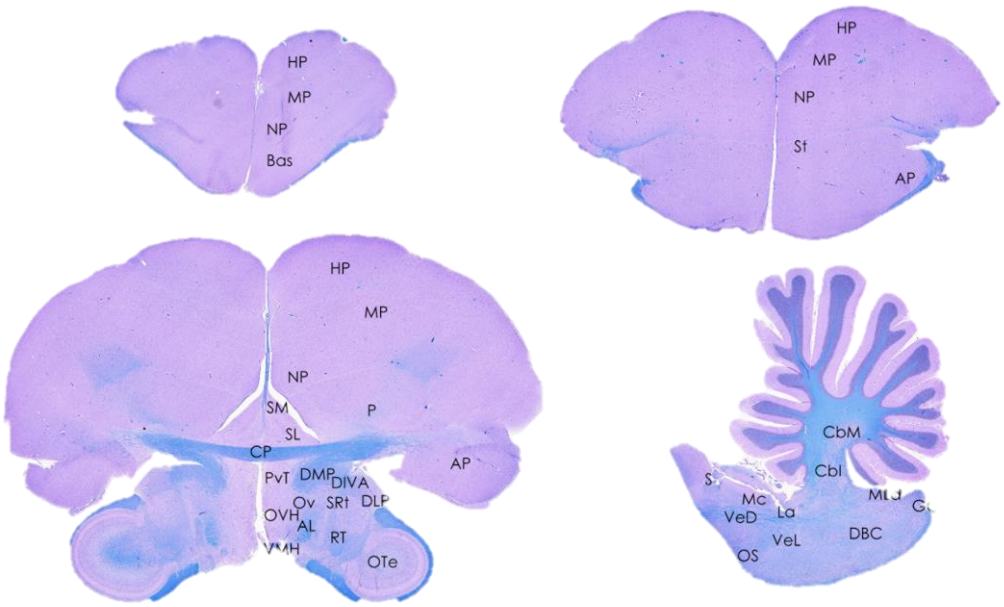

Figure 12. Schematic map for histological landmark orientation in the 4 selected brain levels (I, II, III, IV). See supplementary table for a list of all abbreviations.

Immunohistochemistry

Immunohistochemistry was performed using polyclonal antibodies against a specific region of the PaBV N-protein as previously described,[77] on serial tissue sections, mounted on charged slides, and examined by light microscopy. Due to the intranuclear replication nature of PaBVs, only cells with intranuclear or intranuclear and intracytoplasmic immunolabeling were considered positive. Cells with only intracytoplasmic immunolabeling were considered negative. Immunolabeling was scored as previously described[154] and the progression of positive immunolabeling for each CNS section was recorded in schematic plates. Briefly, slides were scored based on the number of N-protein positive cells in the whole section of brain or spinal cord as follows: - (absent), + (1-3% affected cells), ++ (4-10% affected cells), +++ (11-25% affected cells) and ++++ (more than 25% affected cells).

Results

Inflammatory infiltrate distribution

For infected birds, lymphoplasmacytic inflammation was more prominent in the central core of the brain, mainly in the thalamus (Level III) and brainstem (Level IV) (Figure 4). In the spinal cord, lesions were equally distributed between the three segments with wide distribution between ventral and dorsal horns (Figure 5).

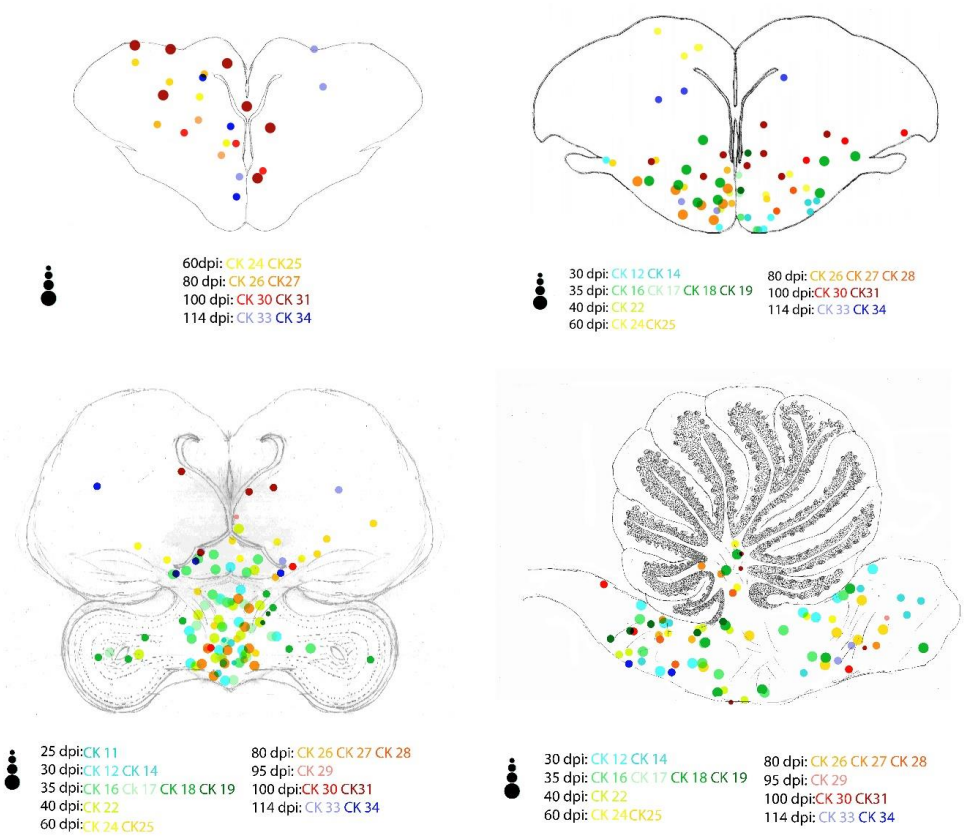

Figure 13. Inflammation distribution and severity across 4 selected levels (I, II, III and IV) of the brain. Inoculated cockatiels with PABV-2 that presented inflammatory lesions are represented by different colors. Each dot represents an inflammatory focus and the four different dot sizes represent different degrees of severity (minimal, mild, moderate and severe).

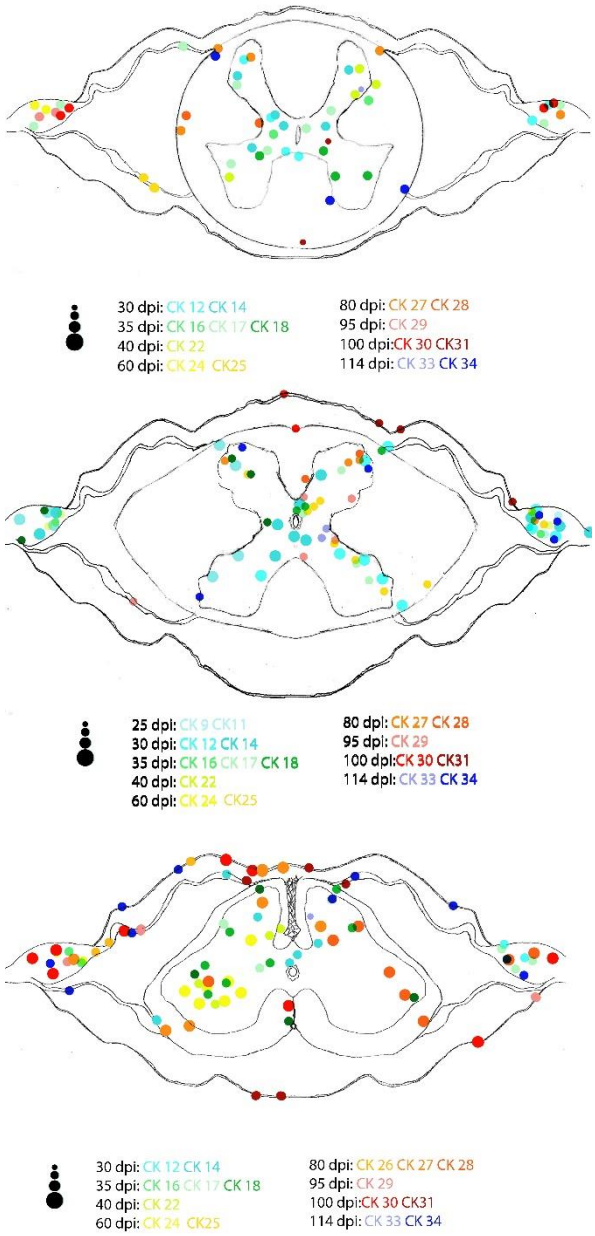

Figure 14. Inflammation distribution and severity across cervical (top), thoracic (middle), and lumbosacral (bottom). Cockatiels that presented inflammatory lesions are represented by different colors. Each dot represents an inflammatory focus and the four different dot sizes represent different degrees of severity (minimal, mild, moderate and severe).

At 25 dpi, the first areas of the brain to present inflammation were the brainstem (level IV) and the thalamus (level III). More specifically, encephalitis was more prominent in the gray matter and first spreading through the nucleus magnocellularis, nucleus olivaris superior and nucleus laminaris in the brainstem and through the paraventricular nucleus of the thalamus. By 30 dpi, inflammation had spread laterally through thalamic nuclei, including the nucleus ovoidalis and nucleus rotundus, and dorsally to the commisura posterior, which was the main region of the white matter affected by inflammation. The nuclei septalis, and scattered areas in the cerebrum at the level of the striatum and nidopallium (level II) were also affected at 30 dpi. At 35 dpi, inflammatory foci reached the optic tectum of the midbrain. Inflammation in the brainstem was consistently present in the areas corresponding to the nucleus olivaris superior, nucleus solitarius, nucleus laminaris, and nucleus decussationis. Out of the 17 cockatiels with inflammation at level IV, only 5 had inflammatory foci in the cerebellum, which only started at 40 dpi and were concentrated at the nucleus cerebellaris intermedius and nucleus cerebellaris internus. Inflammation also reached the most dorsal areas comprising the mesopallium and hyperpallium at 40 dpi affecting both gray and white matter at level II. At level I, the inflammation reached scattered areas in the mesopallium and nidopallium at 60 dpi Sections of level III and level IV continuously presented inflammatory foci throughout 60, 80, 95, 100, until 114 dpi. Interestingly, the cerebrum at the levels I and II did not show inflammation at 95 dpi. At 60, 80, 100 and 114 dpi, inflammatory foci were mainly concentrated in the mesopallium and hyperpallium. Meningitis in the brain was only observed at 60, 100 and 114 dpi, and its severity ranged from minimal to mild.

The first spinal cord segment to develop inflammatory foci was the thoracic spinal cord at 25 dpi. Inflammation was predominant in the ventral horns accompanied by ganglioneuritis until 35 dpi when it started to spread to the dorsal horns. Both cervical and lumbosacral segments of the spinal cord first developed inflammation at 30 dpi affecting both dorsal and ventral horns as well as adjacent spinal ganglia. All sections presented inflammation, primarily in the gray matter throughout all timepoints until 114 dpi. Although less frequent and severe than inflammation in the gray matter, inflammatory foci in the white matter were first observed close to nerve insertions of the ventral funiculus at 30 dpi, followed by the dorsal funiculus at 80 dpi. Then white matter inflammation was more concentrated close to nerve insertions in the ventral, dorsal and lateral funiculi, mostly in the interface of gray and white matter until 114 dpi. No ganglioneuritis was observed at 25 and 114 dpi in the cervical segment, at 95 and 100 dpi in the thoracic, and at 40 dpi in the lumbosacral spinal cord. Ganglioneuritis was more severe and frequent in the latter segment. Meningitis in the spinal cord was only observed at 80, 95, 100 and 114 dpi and it was also more frequent and severe in the lumbosacral segment. No inflammation was observed in the glycogen body.

Viral antigen distribution

Immunolabeling was observed in the nuclei and/or nuclei and cytoplasm of predominantly neurons, but glial and ependymal cells were also intermittently positive (Figure 6). Immunolabeling was observed as early as 20 dpi unilaterally in the neurons and glial cells of the ventral horn and adjacent ganglia of the thoracic spinal cord, and at

25 dpi in the cervical and lumbosacral segments. At 40 dpi, the immunolabeling spread to the ependymal cells, to the adjacent neurons and glial cells including cells in the dorsal horns in all 3 segments of the spinal cord. Immunolabeling in the glial cells of the white matter was first observed at 80 dpi. In all following timepoints (80, 95, 100, 114 dpi), a diffuse labelling involving neurons, glial and ependymal cells in both gray and white matter as well as neurons of the adjacent ganglia, was observed (Figure 7).

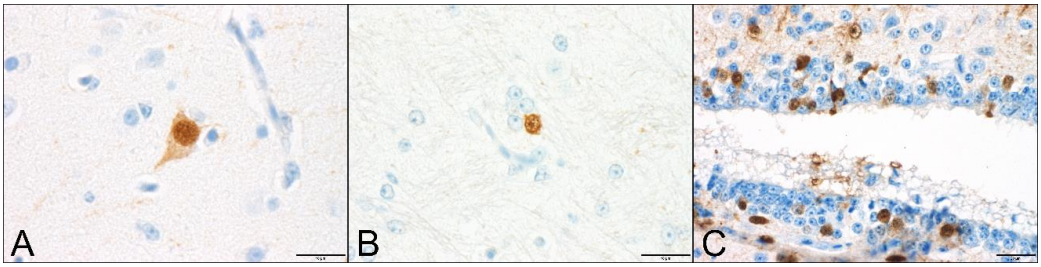

Figure 15. Immunolabeling for PaBV nucleoprotein in neurons (A), glial cells (B), and ependymal cells (C).

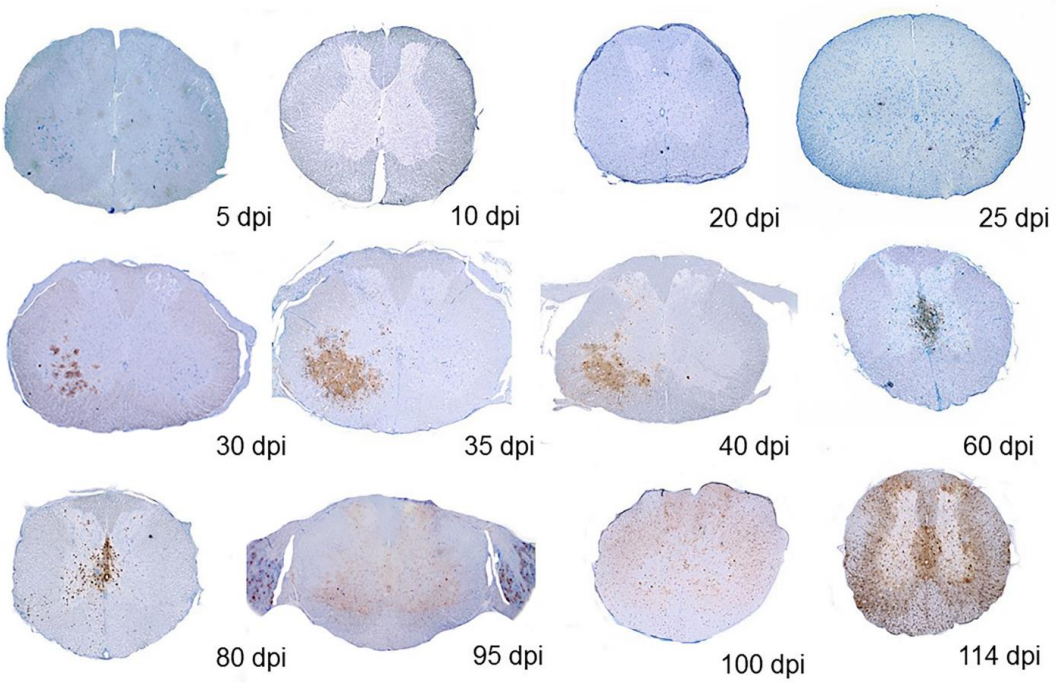

Figure 16. Progression of immunolabeling for PaBV N-protein across all timepoints in the thoracic spinal cord.

In the brain, the thalamic nuclei (level III) and the brainstem (level IV) were simultaneously the first areas of the brain with PaBV immunolabeling at 25 dpi. From 25 to 30 dpi, scattered neurons of the paraventricular nuclei of the thalamus and glial cells scattered throughout the thalamus were positive. At 30 dpi, few neurons of the nucleus basorostralis (level I) and striatum (level II) were positive. At 35 dpi, the labelling rapidly spread throughout the central core reaching the nuclei septalis in the subpallium; and to neurons of the nuclei cereberallis of the molecular layer and also in the granule cell layer of the cerebellum. Ependymal cells were also positive at 35 dpi, particularly in the organum vasculosum of the hypothalamus, surrounding the third ventricle. At 40 dpi, immunolabeling was strongly positive in the pallial areas, particularly prominent in the arcopallium and nidopallium. Also at 40 dpi, PaBV-positive neurons and glial cells were identified in the optic tectum and hyperpallium. At level I, the most widespread immunolabeling for this section only started at 60 dpi. A diffuse pattern affecting virtually all regions of the cerebrum was observed from 60 to 114 dpi. A widespread pattern affecting not only the cerebellar nuclei but also the white matter and the Purkinje cells was first observed at 80 dpi and remained positive until 114 dpi (Figure 8).

No inflammatory foci or antigen immunolabeling were observed in control birds.

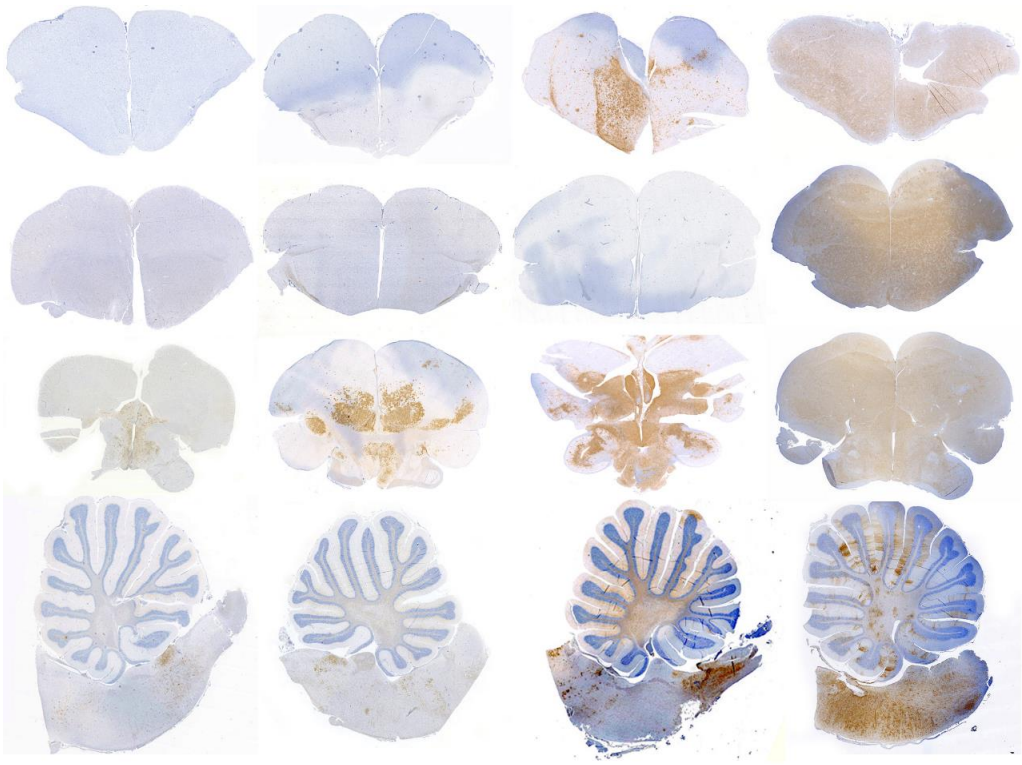

Figure 17. Progression of PaBV immunolabeling for N-protein at 35, 60, 80 and 114 dpi in all 4 selected brain levels.

Discussion

All infected birds experimentally inoculated with PaBV-2 in the pectoral muscle developed a lymphoplasmacytic meningoencephalomyelitis. This was associated with consistent intranuclear immunolabeling of PABV N protein antigen mainly in neurons; compatible with what it has been described in natural cases of PDD.32 Although previous studies have been able to identify PaBV N-protein antigen and inflammatory lesions in the CNS of natural and experimental cases of PDD,[17, 31, 32, 36, 64, 66] the distribution of the inflammation and/or immunolabeling are often only broadly determined with minimal neuroanatomic mapping.[151] In this study, immunolabeling for PaBV N-protein preceded the development of inflammation and the ventral horns of the thoracic spinal cord were the first positive CNS areas at 20 dpi. The brainstem (Level IV) and the thalamus (Level III) were the first areas of the brain to simultaneously present viral antigen and inflammation at 25 dpi. The interval between 25 and 60 dpi was crucial for the viral spread, progressively and consistently affected several areas in both gray and white matter. Timepoints after 60 dpi presented a diffuse and widespread pattern of inflammation and viral antigen distribution throughout the three most caudal areas of the brain. Level I remained as the least affected area until 100 dpi. Additionally, throughout all timepoints, both inflammation and viral distribution were more concentrated to the ventral areas of the brain.

Interestingly, some studies show that experimentally infected cockatiels have gastrointestinal signs prior to developing neurological signs,[32, 120] and ganglioneuritis has been reported as a more consistent finding than meningoencephalomyelitis.[17, 24, 32, 66] Our

results suggest that the common practice of collecting and assessing only a single section of the brain could lead to a false-negative diagnosis in PaBV-infected birds, especially in the early timepoints of infection. We observed that levels III and IV developed inflammation in cockatiels from 9 out of the 12 timepoints (25 to 114 dpi). On the other hand, we only identified lesions in level I in cockatiels from 60, 80, 100 and 114 dpi. Therefore, sampling limited to rostral areas of cerebrum would be prone to miss the vast majority of inflammatory lesions which might result in the misleading assumption that gastrointestinal ganglioneuritis were present prior to the meningoencephalomyelitis.

In this study, the inflammatory lesions bear some similarities to what has been described for mammalian bornaviruses. Lymphoplasmacytic meningoencephalomyelitis with predilection for gray matter, including areas such as the thalamus and hypothalamus, and relatively sparing the cerebellum and dorsal cerebrum was our main histological finding as reported for horses, sheep, variegated squirrels, humans and immunocompetent rodents.[4, 40, 43, 94, 129, 136] Additionally, immunohistochemistry of human and squirrel brain samples infected with VSVB-1 generally follow a pattern affecting the nuclei, cytoplasm, and neuronal and glial processes,[25] similar to that observed in our study.

In contrast, the predilection for olfactory bulb and hippocampus in mammals, a feature that fits the olfactory route of infection proposed for BoDV pathogenesis[145] and follows a rostral-caudal progression of BoDV infection, was not observed in our study. The natural route of infection for PaBVs remains to be elucidated, and while experimental olfactory infection has failed to induce disease in cockatiels,[65] a potential intramuscular route of infection, as reproduced in our experiment,[154] creates the possibility of PaBVs

being spread first to the spinal cord and only reaching the rostral areas of the cerebrum in the late course of infection, which results in a caudal-rostral progression of infection and explains the reduced inflammation and presence of viral N-protein antigen seen in the more rostral areas during the late timepoints.

Although the hippocampus is associated to spatial memory in both birds and mammals, its localization and structure differs enormously between both classes.[155] While in mammals it is located rostral to the midbrain and ventral to the thalamus, the hippocampus in birds has a dorsal localization in the pallial region of the cerebrum.[151] This area was not affected in the cockatiels of this study, probably due the central core predilection of the virus and consequent inflammation concentrated in the ventral areas of the brain. Additionally, birds lack a distinguished dentate gyrus, which makes the progressive cell death for the granule cells reported in the hippocampus of BoDV-infected rats difficult to be assessed in birds.[6, 156]

The pathognomonic feature of mammalian BoDV infection, the eosinophilic intranuclear inclusion bodies known as Joest-Degen bodies,[140] were not observed in this study.[150] Although these inclusion bodies have been reported in few PDD cases,[157-159] demonstration of the inclusion bodies in H&E preparations as observed for mammals[27] has not been consistent and a careful analysis of the morphological and staining characteristics of the inclusion bodies must be taken in consideration to differentiate them from fragmented nucleoli or artifacts.

In conclusion, our results suggest that thalamus and brainstem were considered the most appropriate sections of the brain for sampling to determine PaBV-2 infection spread

and inflammation. Little or no difference was observed between the three segments of the spinal cord in our PaBV-2 experimental study based on distribution of viral antigen and inflammatory lesions. Further research is needed to understand whether a similar process happens in naturally infected birds and elucidate the mode of viral spread from animal to animal as well as to more fully understand the physiologic and behavioral effects of viral and inflammation spread during the infection progression. Additionally, we advocate the processing of the spinal cord with the vertebral bodies in birds, once our results demonstrate the outstanding visualization of the spinal ganglia and the decalcification process did not interfere on viral antigen detection.

CHAPTER V

CONCLUSIONS

Our results have enlightened important aspects of the pathogenesis of bornaviral infections in psittacine birds and PDD.

The lack of evidence of classical PDD clinical signs and lesions after inoculation of gangliosides in quaker parrots as discussed in Chapter II, demonstrates the fragility of the theory that speculates PDD as an autoimmune disease with similar features of GBS. We were able to detect anti-ganglioside antibodies in the inoculated birds, but we were not able to find any evidence of a correlation between these antibodies and PDD.

On the other hand, our experimental inoculations of PaBV-2 in cockatiels successfully filled Koch-s postulates and triggered neurological and gastrointestinal clinical signs commonly seen in PDD, that were supported by macroscopic and/or microscopic lesions , and identification of antigen and viral RNA in tissues. The experiments described in Chapters III and IV bring the causal relationship of PaBV-2 and PDD to light, and reinforce the immunopathological mechanisms involved in the pathogenesis of this devastating disease.

Furthermore, we were able to demonstrate the viral progression of PaBV-2 through 12 different timepoints and its relationship to the development of lesions in early and late infection. The thorough examination of a wide variety of tissues from infected cockatiels by histopathological, immunohistochemical and molecular methods described in Chapter III, was able to list the degree of compromise of different organs and consequently indicated the appropriate tissues for diagnostic evaluation.

Finally, neurotropism is a striking feature of bornaviral infections, which is clearly reflected in PDD. The studies discussed in Chapter IV provide a unique understanding of the distribution of PaBV-2 and the lesions provoked by this virus in the CNS of infected cockatiels. We were able to trace the progression of PaBV-2 and lesions across 4 different sections of the brain and 3 different sections of the spinal cord, which resulted in the understanding of the predilection of PaBV-2 for thalamus and brainstem, and no significant differences was observed across the segments of the spinal cord. These results have an important contribution for the enhancement of the diagnoses and future research of bornaviral infections.

Nevertheless, our results correspond to experimental and controlled conditions, and further research is necessary to understand if our results corroborate with the findings observed across different psittacine species and with natural cases of PDD.

REFERENCES

1. Cubitt B, Oldstone C and de la Torre JC. Sequence and genome organization of Borna disease virus. *J Virol*. 1994; 68: 1382-96.

2. Kuhn JH, Durrwald R, Bao Y, et al. Taxonomic reorganization of the family Bornaviridae. *Arch Virol*. 2015; 160: 621-32.

3. Afonso CL, Amarasinghe GK, Banyai K, et al. Taxonomy of the order Mononegavirales: update 2016. *Arch Virol*. 2016; 161: 2351-60.

4. Tizard I, Ball J, Stoica G and Payne S. The pathogenesis of bornaviral diseases in mammals. *Anim Health Res Rev*. 2016: 1-18.

5. Matsumoto Y, Hayashi Y, Omori H, et al. Bornavirus closely associates and segregates with host chromosomes to ensure persistent intranuclear infection. *Cell Host Microbe*. 2012; 11: 492-503.

6. Mayer D, Fischer H, Schneider U, Heimrich B and Schwemmle M. Borna disease virus replication in organotypic hippocampal slice cultures from rats results in selective damage of dentate granule cells. *J Virol*. 2005; 79: 11716-23.

7. Schwemmle M, Salvatore M, Shi L, Richt J, Lee CH and Lipkin WI. Interactions of the borna disease virus P, N, and X proteins and their functional implications. *J Biol Chem*. 1998; 273: 9007-12.

8. Mirhosseini N, Gray PL, Tizard I and Payne S. Complete genome sequence of avian bornavirus genotype 1 from a Macaw with proventricular dilatation disease. *J Virol*. 2012; 86: 7023.

9. Schwemmle M and Lipkin WI. Models and mechanisms of Bornavirus pathogenesis. *Drug Discovery Today: Disease Mechanisms*. 2004; 1: 211-6.

10. de la Torre JC. Reverse-genetic approaches to the study of Borna disease virus. *Nat Rev Micro*. 2006; 4: 777-83.

11. Musser JM, Heatley JJ, Koinis AV, et al. Ribavirin Inhibits Parrot Bornavirus 4 Replication in Cell Culture. *Plos One*. 2015; 10: e0134080.

12. Horie M, Kobayashi Y, Suzuki Y and Tomonaga K. Comprehensive analysis of endogenous bornavirus-like elements in eukaryote genomes. *Philos Trans R Soc Lond B Biol Sci*. 2013; 368: 20120499.

13. Tomonaga K, Kobayashi T and Ikuta K. Molecular and cellular biology of Borna disease virus infection. *Microbes Infect*. 2002; 4: 491-500.

14. Cros JF and Palese P. Trafficking of viral genomic RNA into and out of the nucleus: influenza, Thogoto and Borna disease viruses. *Virus Res*. 2003; 95: 3-12.

15. Herrel M, Hoefs N, Staeheli P and Schneider U. Tick-borne Nyamanini virus replicates in the nucleus and exhibits unusual genome and matrix protein properties. *J Virol*. 2012; 86: 10739-47.

16. Clark FD. Proventricular dilatation syndrome in large psittacine birds. *Avian Dis*. 1984; 28: 813-5.

17. Piepenbring AK, Enderlein D, Herzog S, et al. Pathogenesis of avian bornavirus in experimentally infected cockatiels. *Emerg Infect Dis*. 2012; 18: 234-41.

18. Honkavuori KS, Shivaprasad HL, Williams BL, et al. Novel borna virus in psittacine birds with proventricular dilatation disease. *Emerg Infect Dis*. 2008; 14.

19. Kistler AL, Gancz A, Clubb S, et al. Recovery of divergent avian bornaviruses from cases of proventricular dilatation disease: Identification of a candidate etiologic agent. *Virol J*. 2008; 5.

20. Payne S, Covaleda L, Jianhua G, et al. Detection and characterization of a distinct bornavirus lineage from healthy Canada geese (Branta canadensis). *J Virol*. 2011; 85: 12053-6.

21. Guo J and Tizard I. The genome sequence of parrot bornavirus 5. *Virus Genes*. 2015; 51: 430-3.

22. Guo J, Baroch J, Randall A and Tizard I. Complete Genome Sequence of an Avian Bornavirus Isolated from a Healthy Canadian Goose (Branta canadensis). *Genome Announc*. 2013; 1.

23. Guo J, Shivaprasad HL, Rech RR, Heatley JJ, Tizard I and Payne S. Characterization of a new genotype of avian bornavirus from wild ducks. *Virol J*. 2014; 11: 197.

24. Rubbenstroth D, Schmidt V, Rinder M, Legler M, Corman VM and Staeheli P. Discovery of a new avian bornavirus genotype in estrildid finches (Estrildidae) in Germany. *Vet Microbiol*. 2014; 168: 318-23.

25. Hoffmann B, Tappe D, Hoper D, et al. A Variegated Squirrel Bornavirus Associated with Fatal Human Encephalitis. *N Engl J Med*. 2015; 373: 154-62.

26. Amarasinghe GK, Bao Y, Basler CF, et al. Taxonomy of the order Mononegavirales: update 2017. *Arch Virol*. 2017; 162: 2493-504.

27. Weissenbock H, Bakonyi T, Sekulin K, et al. Avian bornaviruses in psittacine birds from Europe and Australia with proventricular dilatation disease. *Emerg Infect Dis*. 2009; 15: 1453-9.

28. Staeheli P, Rinder M and Kaspers B. Avian bornavirus associated with fatal disease in psittacine birds. *J Virol*. 2010; 84: 6269-75.

29. Rinder M, Ackermann A, Kempf H, Kaspers B, Korbel R and Staeheli P. Broad tissue and cell tropism of avian bornavirus in parrots with proventricular dilatation disease. *J Virol*. 2009; 83: 5401-7.

30. de Kloet AH, Kerski A and de Kloet SR. Diagnosis of Avian bornavirus infection in psittaciformes by serum antibody detection and reverse transcription polymerase chain reaction assay using feather calami. *J Vet Diagn Invest*. 2011; 23: 421-9.

31. Payne S, Shivaprasad HL, Mirhosseini N, et al. Unusual and severe lesions of proventricular dilatation disease in cockatiels (Nymphicus hollandicus) acting as healthy carriers of avian bornavirus (ABV) and subsequently infected with a virulent strain of ABV. *Avian Pathol*. 2011; 40: 15-22.

32. Piepenbring AK, Enderlein D, Herzog S, et al. Parrot Bornavirus (PaBV)-2 isolate causes different disease patterns in cockatiels than PaBV-4. *Avian Pathol*. 2016; 45: 156-68.

33. Heffels-Redmann U, Enderlein D, Herzog S, et al. Follow-up investigations on different courses of natural avian bornavirus infections in psittacines. *Avian Dis*. 2012; 56: 153-9.

34. Heffels-Redmann U, Enderlein D, Herzog S, et al. Occurrence of avian bornavirus infection in captive psittacines in various European countries and its association with proventricular dilatation disease. *Avian Pathol*. 2011; 40: 419-26.

35. Gancz AY, Kistler AL, Greninger AL, et al. Experimental induction of proventricular dilatation disease in cockatiels (Nymphicus hollandicus) inoculated with brain homogenates containing avian bornavirus 4. *Virol J*. 2009; 6: 100.

36. Gray P, Hoppes S, Suchodolski P, et al. Use of avian bornavirus isolates to induce proventricular dilatation disease in conures. *Emerg Infect Dis*. 2010; 16: 473-9.

37. Mirhosseini N, Gray PL, Hoppes S, Tizard I, Shivaprasad HL and Payne S. Proventricular dilatation disease in cockatiels (Nymphicus hollandicus) after infection with a genotype 2 avian bornavirus. *J Avian Med Surg*. 2011; 25: 199-204.

38. Encinas-Nagel N, Enderlein D, Piepenbring A, et al. Avian bornavirus in free-ranging psittacine birds, Brazil. *Emerg Infect Dis*. 2014; 20: 2103-6.

39. Tizard I, Shivaprasad HL, Guo J, Hameed S, Ball J and Payne S. The pathogenesis of proventricular dilatation disease. *Anim Health Res Rev*. 2016; 17: 110-26.

40. Gosztonyi G. Natural and experimental Borna disease virus infections--neuropathology and pathogenetic considerations. *APMIS Suppl*. 2008: 53-7.

41. Gosztonyi G and Ludwig H. Borna disease--neuropathology and pathogenesis. *Curr Top Microbiol Immunol*. 1995; 190: 39-73.

42. Baruch K and Schwartz M. CNS-specific T cells shape brain function via the choroid plexus. *Brain Behav Immun*. 2013; 34: 11-6.

43. Sobbe M, Bilzer T, Gommel S, Noske K, Planz O and Stitz L. Induction of degenerative brain lesions after adoptive transfer of brain lymphocytes from Borna disease virus-infected rats: presence of CD8+ T cells and perforin mRNA. *J Virol*. 1997; 71: 2400-7.

44. Rott O, Herzog S and Cash E. T cell memory specific for self and non-self antigens in rats persistently infected with Borna disease virus. *Clin Exp Immunol*. 1993; 93: 370-6.

45. Rott R and Becht H. Natural and experimental Borna disease in animals. *Curr Top Microbiol Immunol*. 1995; 190: 17-30.

46. Stitz L, Soeder D, Deschl U, Frese K and Rott R. Inhibition of immune-mediated meningoencephalitis in persistently Borna disease virus-infected rats by cyclosporine A. *J Immunol*. 1989; 143: 4250-6.

47. Stitz L, Richt JA and Rott R. [Immunopathogenesis of Borna disease]. *Tierarztl Prax*. 1991; 19: 267-70.

48. Noske K, Bilzer T, Planz O and Stitz L. Virus-specific CD4+ T cells eliminate borna disease virus from the brain via induction of cytotoxic CD8+ T cells. *J Virol*. 1998; 72: 4387-95.

49. Hatalski CG, Hickey WF and Lipkin WI. Humoral immunity in the central nervous system of Lewis rats infected with Borna disease virus. *J Neuroimmunol*. 1998; 90: 128-36.

50. Walsh JT, Watson N and Kipnis J. T cells in the central nervous system: messengers of destruction or purveyors of protection? *Immunology*. 2014; 141: 340-4.

51. Ovanesov MV, Sauder C, Rubin SA, et al. Activation of microglia by borna disease virus infection: in vitro study. *J Virol*. 2006; 80: 12141-8.

52. Ovanesov MV, Moldovan K, Smith K, Vogel MW and Pletnikov MV. Persistent Borna Disease Virus (BDV) infection activates microglia prior to a detectable loss of granule cells in the hippocampus. *J Neuroinflammation*. 2008; 5: 16.

53. Ovanesov MV, Ayhan Y, Wolbert C, Moldovan K, Sauder C and Pletnikov MV. Astrocytes play a key role in activation of microglia by persistent Borna disease virus infection. *J Neuroinflammation*. 2008; 5: 50.

54. Weissenbock H, Hornig M, Hickey WF and Lipkin WI. Microglial activation and neuronal apoptosis in Bornavirus infected neonatal Lewis rats. *Brain Pathol*. 2000; 10: 260-72.

55. Coulter DA and Eid T. Astrocytic regulation of glutamate homeostasis in epilepsy. *Glia*. 2012; 60: 1215-26.

56. Vesce S, Rossi D, Brambilla L and Volterra A. Glutamate release from astrocytes in physiological conditions and in neurodegenerative disorders characterized by neuroinflammation. *Int Rev Neurobiol*. 2007; 82: 57-71.

57. Choi DW. Glutamate neurotoxicity and diseases of the nervous system. *Neuron*. 1988; 1: 623-34.

58. Peng XQ, Li X, Gilbert JG, et al. Gamma-vinyl GABA inhibits cocaine-triggered reinstatement of drug-seeking behavior in rats by a non-dopaminergic mechanism. *Drug Alcohol Depend*. 2008; 97: 216-25.

59. Makino A, Fujino K, Parrish NF, Honda T and Tomonaga K. Borna disease virus possesses an NF-kB inhibitory sequence in the nucleoprotein gene. *Sci Rep*. 2015; 5: 8696.

60. Bonnaud EM, Szelechowski M, Betourne A, et al. Borna disease virus phosphoprotein modulates epigenetic signaling in neurons to control viral replication. *J Virol*. 2015; 89: 5996-6008.

61. de la Torre JC. Bornavirus and the Brain. *Journal of Infectious Diseases*. 2002; 186: S241-S7.

62. Tomonaga K. [Borna disease virus: its broad host range and neuropathogenesis]. *Uirusu*. 2002; 52: 41-6.

63. Lundgren AL, Zimmermann W, Bode L, et al. Staggering disease in cats: isolation and characterization of the feline Borna disease virus. *J Gen Virol*. 1995; 76 (Pt 9): 2215-22.

64. Rubbenstroth D, Brosinski K, Rinder M, et al. No contact transmission of avian bornavirus in experimentally infected cockatiels (Nymphicus hollandicus) and domestic canaries (Serinus canaria forma domestica). *Vet Microbiol*. 2014; 172: 146-56.

65. Heckmann J, Enderlein D, Piepenbring AK, et al. Investigation of Different Infection Routes of Parrot Bornavirus in Cockatiels. *Avian Dis*. 2017; 61: 90-5.

66. Gancz AY, Kistler AL, Greninger AL, et al. Experimental induction of proventricular dilatation disease in cockatiels (Nymphicus hollandicus) inoculated with brain homogenates containing avian bornavirus 4. *Virology Journal*. 2009; 6: 100.

67. Vondrackova M, Tukac V, Grymova V, Hajkova P, Knotek Z and Dorrestein GM. Detection of anti-avian bornavirus antibodies in parrots in the Czech Republic and Slovakia. *Acta Vet Brno*. 2014; 83: 195-9.

68. Villanueva I, Gray P, Mirhosseini N, et al. The diagnosis of proventricular dilatation disease: Use of a Western blot assay to detect antibodies against avian Borna virus. *Veterinary Microbiology*. 2010; 143: 196-201.

69. Herzog S, Enderlein D, Heffels-Redmann U, et al. Indirect immunofluorescence assay for intra vitam diagnosis of avian bornavirus infection in psittacine birds. *J Clin Microbiol*. 2010; 48: 2282-4.

70. Hoppes SM, Tizard I and Shivaprasad HL. Avian bornavirus and proventricular dilatation disease: diagnostics, pathology, prevalence, and control. *Vet Clin North Am Exot Anim Pract*. 2013; 16: 339-55.

71. Murray O, Turner D, Streeter K, et al. Apparent resolution of parrot bornavirus infection in cockatiels (Nymphicus hollandicus). *Vet Med-Res Rep*. 2017; 8: 31-6.

72. Mannl A, Gerlach H and Leipold R. Neuropathic gastric dilatation in psittaciformes. *Avian Dis*. 1987; 31: 214-21.

73. Raghav R, Taylor M, Delay J, et al. Avian bornavirus is present in many tissues of psittacine birds with histopathologic evidence of proventricular dilatation disease. *J Vet Diagn Invest*. 2010; 22: 495-508.

74. Wunschmann A, Honkavuori K, Briese T, Lipkin WI, Shivers J and Armien AG. Antigen tissue distribution of Avian bornavirus (ABV) in psittacine birds with natural

spontaneous proventricular dilatation disease and ABV genotype 1 infection. *J Vet Diagn Invest*. 2011; 23: 716-26.

75. Ouyang N, Storts R, Tian Y, et al. Histopathology and the detection of avian bornavirus in the nervous system of birds diagnosed with proventricular dilatation disease. *Avian Pathol*. 2009; 38: 393-401.

76. Delnatte P, Mak M, Ojkic D, Raghav R, DeLay J and Smith DA. Detection of Avian bornavirus in multiple tissues of infected psittacine birds using real-time reverse transcription polymerase chain reaction. *J Vet Diagn Invest*. 2014; 26: 266-71.

77. Leal de Araujo J, Plumlee Q, Rech RR, Winkel-Blair A, Hoppes S and Schneider SM. Proventricular rupture associated with Psittaciforme 1 Bornavirus (PaBV) infection in a Major Mitchell Cockatoo (Lophochroa leadbeateri). *Brazilian Journal of Veterinary Pathology*. 2016; 9.

78. Rossi G, Crosta L and Pesaro S. Parrot proventricular dilation disease. *Vet Rec*. 2008; 163: 310.

79. Nachamkin I, Allos BM and Ho T. Campylobacter Species and Guillain-Barré Syndrome. *Clinical Microbiology Reviews*. 1998; 11: 555-67.

80. Van den Berg B, Walgaard C, Drenthen J, Fokke C, Jacobs BC and van Doorn PA. Guillain-Barre syndrome: pathogenesis, diagnosis, treatment and prognosis. *Nat Rev Neurol*. 2014; 10: 469-82.

81. Nyati K and Nyati R. Role of Campylobacter jejuni infection in the pathogenesis of Guillain-Barre syndrome: an update. *Biomed Res Int*. 2013; 2013: 852195.

82. dos Santos T, Rodriguez A, Almiron M, et al. Zika Virus and the Guillain–Barré Syndrome — Case Series from Seven Countries. *New Engl J Med*. 2016; 375: 1598-601.

83. Venkatesan A and Benavides DR. Autoimmune encephalitis and its relation to infection. *Curr Neurol Neurosci Rep*. 2015; 15: 3.

84. Oehler E, Watrin L, Larre P, et al. Zika virus infection complicated by Guillain-Barre syndrome--case report, French Polynesia, December 2013. *Euro Surveill*. 2014; 19.

85. Yu RK, Ariga T, Yanagisawa M and Zeng G. Gangliosides in the Nervous System: Biosynthesis and Degradation. In: Fraser-Reid B, Tatsuta K and Thiem J, (eds.). *Glycoscience*. Springer Berlin Heidelberg, 2008, p. 1671-95.

86. Yu RK, Usuki S and Ariga T. Ganglioside Molecular Mimicry and Its Pathological Roles in Guillain-Barré Syndrome and Related Diseases. *Infection and Immunity*. 2006; 74: 6517-27.

87. Svennerholm L and Fredman P. A procedure for the quantitative isolation of brain gangliosides. *Biochimica et Biophysica Acta*. 1980; 617: 97-109.

88. Pesaro S, Crosta L, Bertoni P, Ceccherelli R and Rossi G. Anti-ganglioside antibodies production as a theory of PDD pathogenesis. *Proc Euro Assoc Avian Vet*. 2009.

89. Guo J, Payne S, Zhang S, Turner D, Tizard I and Suchodolski P. Avian bornaviruses: diagnosis, isolation, and genotyping. *Curr Protoc Microbiol*. 2014; 34: 15I 1 1-33.

90. Millar HR, Simpson JG and Stalker AL. An evaluation of the heat precipitation method for plasma fibrinogen estimation. *J Clin Pathol*. 1971; 24: 827-30.

91. Towbin H, Staehelin T and Gordon J. Electrophoretic transfer of proteins from polyacrylamide gels to nitrocellulose sheets: procedure and some applications. *Proceedings of the National Academy of Sciences*. 1979; 76: 4350-4.

92. Alaedini A, Green PH, Sander HW, et al. Ganglioside reactive antibodies in the neuropathy associated with celiac disease. *J Neuroimmunol*. 2002; 127: 145-8.

93. Riggott MJ and Matthew WD. Anti-idiotypic monoclonal antibodies to GM1 identify ganglioside binding proteins. *Glycobiology*. 1996; 6: 581-9.

94. Hallensleben W, Schwemmle M, Hausmann J, et al. Borna disease virus-induced neurological disorder in mice: infection of neonates results in immunopathology. *J Virol*. 1998; 72: 4379-86.

95. Graham D. Wasting/proventricular dilatation disease: a pathologist's view. *Proceedings of the Annual Conference of the Association of Avian Veterinarians Association of Avian Veterinarians, Lake Worth, TX*. InR, 1991, p. 43-4.

96. Casteleyn C, Doom M, Lambrechts E, Van den Broeck W, Simoens P and Cornillie P. Locations of gut-associated lymphoid tissue in the 3-month-old chicken: a review. *Avian Pathol*. 2010; 39: 143-50.

97. Abdul-Aziz T, Fletcher OJ, Barnes HJ, Shivaprasad HL, Swayne DE and American Association of Avian P. *Avian histopathology*. 4th edition. ed. Jacksonville, Florida :: American Association of Avian Pathologists, 2016.

98. Gancz D and Fishelson Z. Cancer resistance to complement-dependent cytotoxicity (CDC): Problem-oriented research and development. *Mol Immunol*. 2009; 46: 2794-800.

99. Lierz M, Hafez HM, Honkavuori KS, et al. Anatomical distribution of avian bornavirus in parrots, its occurrence in clinically healthy birds and ABV-antibody detection. *Avian Pathol*. 2009; 38: 491-6.

100. Encinas-Nagel N, Enderlein D, Piepenbring A, et al. Avian Bornavirus in Free-Ranging Psittacine Birds, Brazil. *Emerging Infectious Diseases*. 2014; 20: 2103-6.

101. Kistler AL, Smith JM, Greninger AL, DeRisi JL and Ganem D. Analysis of Naturally Occurring Avian Bornavirus Infection and Transmission during an Outbreak of Proventricular Dilatation Disease among Captive Psittacine Birds. *J Virol*. 2010; 84: 2176-9.

102. Berhane Y, Smith DA, Newman S, et al. Peripheral neuritis in psittacine birds with proventricular dilatation disease. *Avian Pathol*. 2001; 30: 563-70.

103. Shin T, Ahn M, Matsumoto Y and Moon C. Mechanism of experimental autoimmune neuritis in Lewis rats: the dual role of macrophages. *Histol Histopathol*. 2013; 28: 679-84.

104. Dornmair K, Goebels N, Weltzien H-U, Wekerle H and Hohlfeld R. T-Cell-Mediated Autoimmunity: Novel Techniques to Characterize Autoreactive T-Cell Receptors. *The American Journal of Pathology*. 2003; 163: 1215-26.

105. Wucherpfennig KW. Mechanisms for the induction of autoimmunity by infectious agents. *Journal of Clinical Investigation*. 2001; 108: 1097-104.

106. Hausmann J, Schamel K and Staeheli P. CD8(+) T lymphocytes mediate Borna disease virus-induced immunopathology independently of perforin. *J Virol*. 2001; 75: 10460-6.

107. Planz O, Bilzer T and Stitz L. Immunopathogenic role of T-cell subsets in Borna disease virus-induced progressive encephalitis. *J Virol*. 1995; 69: 896-903.

108. Richt JA, Schmeel A, Frese K, Carbone KM, Narayan O and Rott R. Borna disease virus-specific T cells protect against or cause immunopathological Borna disease. *J Exp Med*. 1994; 179: 1467-73.

109. Schmidt B, Toyka KV, Kiefer R, Full J, Hartung HP and Pollard J. Inflammatory infiltrates in sural nerve biopsies in Guillain-Barre syndrome and chronic inflammatory demyelinating neuropathy. *Muscle Nerve*. 1996; 19: 474-87.

110. Asbury AK, Arnason BG and Adams RD. Inflammatory Lesion in Idiopathic Polyneuritis - Its Role in Pathogenesis. *Medicine*. 1969; 48: 173-&.

111. Griffin JW, Li CY, Ho TW, et al. Pathology of the motor-sensory axonal Guillain-Barre syndrome. *Ann Neurol*. 1996; 39: 17-28.

112. Prineas JW. Acute Idiopathic Polyneuritis - Electron-Microscope Study. *Lab Invest*. 1972; 26: 133-&.

113. Staeheli P, Rinder M and Kaspers B. Avian Bornavirus Associated with Fatal Disease in Psittacine Birds. *J Virol*. 2010; 84: 6269-75.

114. Gancz AY, Kistler AL, Greninger AL, et al. Experimental induction of proventricular dilatation disease in cockatiels (Nymphicus hollandicus) inoculated with brain homogenates containing avian bornavirus 4. *Virology Journal*. 2009; 6.

115. Gray P, Hoppes S, Suchodolski P, et al. Use of Avian Bornavirus Isolates to Induce Proventricular Dilatation Disease in Conures (vol 16, pg 473, 2010). *Emerging Infectious Diseases*. 2010; 16: 750-.

116. Rubbenstroth D, Schmidt V, Rinder M, et al. Phylogenetic Analysis Supports Horizontal Transmission as a Driving Force of the Spread of Avian Bornaviruses. *Plos One*. 2016; 11: e0160936.

117. Moses PL, Ellis LM, Anees MR, et al. Antineuronal antibodies in idiopathic achalasia and gastro-oesophageal reflux disease. *Gut*. 2003; 52: 629-36.

118. Storch WB. [Autoantibodies against podocytes of the kidney glomerulus]. *Immun Infekt*. 1995; 23: 25-6.

119. Tappe D, Schmidt-Chanasit J and Beer M. Bornavirus Associated with Fatal Human Encephalitis. *N Engl J Med*. 2015; 373: 1880-1.

120. Piepenbring AK, Enderlein D, Herzog S, et al. Pathogenesis of Avian Bornavirus in Experimentally Infected Cockatiels. *Emerging Infectious Diseases*. 2012; 18: 234-41.

121. Rubbenstroth D, Brosinski K, Rinder M, et al. No contact transmission of avian bornavirus in experimentally infected cockatiels (Nymphicus hollandicus) and domestic canaries (Serinus canaria forma domestica). *Vet Microbiol*. 2014; 172: 146-56.

122. Olbert M, Romer-Oberdorfer A, Herden C, et al. Viral vector vaccines expressing nucleoprotein and phosphoprotein genes of avian bornaviruses ameliorate homologous challenge infections in cockatiels and common canaries. *Sci Rep*. 2016; 6: 36840.

123. Runge S, Olbert M, Herden C, et al. Viral vector vaccines protect cockatiels from inflammatory lesions after heterologous parrot bornavirus 2 challenge infection. *Vaccine*. 2017; 35: 557-63.

124. Guo J, Payne S, Zhang S, Turner D, Tizard I and Suchodolski P. Avian Bornaviruses: Diagnosis, Isolation, and Genotyping. *Current Protocols in Microbiology*. John Wiley & Sons, Inc., 2005.

125. Rubbenstroth D, Rinder M, Stein M, et al. Avian bornaviruses are widely distributed in canary birds (Serinus canaria f. domestica). *Vet Microbiol*. 2013; 165: 287-95.

126. Schlottau K, Jenckel M, van den Brand J, et al. Variegated Squirrel Bornavirus 1 in Squirrels, Germany and the Netherlands. *Emerg Infect Dis*. 2017; 23: 477-81.

127. Salinas S, Schiavo G and Kremer EJ. A hitchhiker's guide to the nervous system: the complex journey of viruses and toxins. *Nat Rev Microbiol*. 2010; 8: 645-55.

128. Hemachudha T, Ugolini G, Wacharapluesadee S, Sungkarat W, Shuangshoti S and Laothamatas J. Human rabies: neuropathogenesis, diagnosis, and management. *Lancet Neurol*. 2013; 12: 498-513.

129. Ludlow M, Kortekaas J, Herden C, et al. Neurotropic virus infections as the cause of immediate and delayed neuropathology. *Acta Neuropathol*. 2016; 131: 159-84.

130. Herden C, Briese T, Lipkin M and Richt J. Bornaviridae. In: Knipe D and Howley P, (eds.). *Fields virology*. Philadelphia: Lippincott Williams & Wilkins, 2013, p. 1124-50.

131. Nobach D, Bourg M, Herzog S, et al. Shedding of Infectious Borna Disease Virus-1 in Living Bicolored White-Toothed Shrews. *PLoS One*. 2015; 10: e0137018.

132. Dietzel J, Kuhrt H, Stahl T, et al. Morphometric analysis of the retina from horses infected with the Borna disease virus. *Vet Pathol*. 2007; 44: 57-63.

133. Rhoades RE, Tabor-Godwin JM, Tsueng G and Feuer R. Enterovirus infections of the central nervous system. *Virology*. 2011; 411: 288-305.

134. Mabbott NA and MacPherson GG. Prions and their lethal journey to the brain. *Nat Rev Microbiol*. 2006; 4: 201-11.

135. Philadelpho NA, Rubbenstroth D, Guimaraes MB and Piantino Ferreira AJ. Survey of bornaviruses in pet psittacines in Brazil reveals a novel parrot bornavirus. *Vet Microbiol*. 2014; 174: 584-90.

136. Watanabe M, Lee BJ, Kamitani W, et al. Neurological diseases and viral dynamics in the brains of neonatally borna disease virus-infected gerbils. *Virology*. 2001; 282: 65-76.

137. Staeheli P, Sauder C, Hausmann J, Ehrensperger F and Schwemmle M. Epidemiology of Borna disease virus. *J Gen Virol*. 2000; 81: 2123-35.

138. Hilbe M, Herrsche R, Kolodziejek J, Nowotny N, Zlinszky K and Ehrensperger F. Shrews as reservoir hosts of borna disease virus. *Emerg Infect Dis*. 2006; 12: 675-7.

139. Murphy FA, Gibbs EPJ, Horzinek MC and Studdert MJ. *Veterinary Virology*. Elsevier Science, 1999.

140. Bestetti G. [Microscopic and ultrastructural studies on Joest-Degen inclusion bodies in spontaneous Borna disease of the horse]. *Schweiz Arch Tierheilkd*. 1976; 118: 493-8.

141. Bilzer T, Grabner A and Stitz L. [Immunopathology of Borna disease in the horse: clinical, virological and neuropathologic findings]. *Tierarztl Prax*. 1996; 24: 567-76.

142. Nowotny N, Kolodziejek J, Jehle CO, Suchy A, Staeheli P and Schwemmle M. Isolation and characterization of a new subtype of Borna disease virus. *J Virol*. 2000; 74: 5655-8.

143. Hornig M, Solbrig M, Horscroft N, Weissenböck H and Lipkin WI. Borna disease virus infection of adult and neonatal rats: Models for neuropsychiatric disease. *Current Topics in Microbiology and Immunology*. 2001, p. 157-77.

144. Carbone KM, Duchala CS and Narayan O. Borna Disease Virus and Antigens in Glial and Neuronal Cell-Populations of the Nervous-System. *Ann Neurol*. 1988; 24: 476-
.

145. Carbone KM. Borna disease virus and human disease. *Clin Microbiol Rev*. 2001; 14: 513-+.

146. Carbone KM, Moench TR and Lipkin WI. Borna Disease Virus Replicates in Astrocytes, Schwann-Cells and Ependymal Cells in Persistently Infected-Rats - Location of Viral Genomic and Messenger-Rnas by Insitu Hybridization. *J Neuropath Exp Neur*. 1991; 50: 205-14.

147. Carbone KM, Trapp BD, Griffin JW, Duchala CS and Narayan O. Astrocytes and Schwann-Cells Are Virus-Host Cells in the Nervous-System of Rats with Borna Disease. *J Neuropath Exp Neur*. 1989; 48: 631-44.

148. Wunschmann A, Honkavuori K, Briese T, Lipkin WI, Shivers J and Armien AG. Antigen tissue distribution of Avian bornavirus (ABV) in psittacine birds with natural spontaneous proventricular dilatation disease and ABV genotype 1 infection. *J Vet Diagn Invest*. 2011; 23: 716-26.

149. Ouyang N, Storts R, Tian Y, et al. Histopathology and the detection of avian bornavirus in the nervous system of birds diagnosed with proventricular dilatation disease. *Avian Pathol*. 2009; 38: 393-401.

150. Raghav R, Taylor M, Delay J, et al. Avian bornavirus is present in many tissues of psittacine birds with histopathologic evidence of proventricular dilatation disease. *J Vet Diagn Invest*. 2010; 22: 495-508.

151. Jarvis ED, Gunturkun O, Bruce L, et al. Avian brains and a new understanding of vertebrate brain evolution. *Nat Rev Neurosci*. 2005; 6: 151-9.

152. Reiner A, Perkel DJ, Bruce LL, et al. The Avian Brain Nomenclature Forum: Terminology for a New Century in Comparative Neuroanatomy. *J Comp Neurol*. 2004; 473: E1-E6.

153. Reiner A. A new avian brain nomenclature: why, how and what. *Brain Res Bull*. 2005; 66: 317-31.

154. Leal de Araujo J, Rech RR, Heatley J, et al. From nerves to brain to gastrointestinal tract: A time-based study of Psittaciform 1 bornavirus (PaBV) pathogenesis in cockatiels (Nymphicus hollandicus). *PLoS One*. 2017; In press.

155. Striedter GF. Evolution of the hippocampus in reptiles and birds. *J Comp Neurol*. 2016; 524: 496-517.

156. Kempermann G. New neurons for 'survival of the fittest'. *Nat Rev Neurosci*. 2012; 13: 727-36.

157. Bourque L, Laniesse D, Beaufrere H, Pastor A, Ojkic D and Smith DA. Identification of avian bornavirus in a Himalayan monal (Lophophorus impejanus) with neurological disease. *Avian Pathol*. 2015; 44: 323-7.

158. Gray P, Hoppes S, Suchodolski P, et al. Use of Avian Bornavirus Isolates to Induce Proventricular Dilatation Disease in Conures. *Emerging Infectious Diseases*. 2010; 16: 473-9.

159. Weissenbock H, Bago Z, Kolodziejek J, et al. Infections of horses and shrews with Bornaviruses in Upper Austria: a novel endemic area of Borna disease. *Emerg Microbes Infect*. 2017; 6: e52.

APPENDIX A

SUPPLEMENTARY TABLE

List of abbreviations

AL	Ansa lenticularis
AP	Arcopallium
Bas	Nucleus basorostralis
CbI	Nucleus cerebellaris internus
CbM	Nucleus cerebellaris intermedius
CP	Comissura posterior
DBC	Nucleus decussationis brachiorum conjunctivorum
DIVA	Dorsalis intermedius pars ventralis anterior
DLP	Nucleus dorsolateralis posterior thalami
DMP	Nucleus dorsomedialis posterior thalami
GCt	Substantia grisea centralis
HP	Hyperpallium
La	Nucleus laminaris
Mc	Nucleus magnocellularis
MLd	Nucleus mesencephalicus lateralis
MP	Mesopallium
NP	Nidopallium
OS	Nucleus olivaris superior
Ote	Optic tectum
Ov	Nucleus ovoidalis
OVH	Organum vasculosum of the hypothalamus
P	Pallidum
PvT	Paraventricular nuclei of the thalamus
Rt	Nucleus rotundus
S	Nucleus solitarius
SL	Nucleus septalis lateralis
SM	Nucleus septalis medialis
SRt	Nucleus subrotundus
St	Striatum
VeD	Nucleus vestibularis descendens
VeL	Nucleus vestibularis lateralis
VMH	Ventromedial nucleus of hypothalamus